Dispersion of heavy particle sets in isotropic turbulence using kinematic simulation

A. Abou El-Azm Aly and F. Nicolleau*
Department of Mechanical Engineering, The University of Sheffield, Sheffield S1 3JD, United Kingdom
(Received 29 January 2008; published 22 July 2008)

We study the dispersion of heavy particle sets, triangle and tetrahedron, in an isotropic and incompressible three-dimensional turbulent flow. The turbulent velocity field is generated using kinematic simulation, which allows us to vary the inertial range and to reach large values of the Reynolds numbers. We study the time evolution of the parameters characterizing the geometry, the size and shape of the triangle and tetrahedron. The Lagrangian correlations of the sets' size, area or volume, are also studied. Different initial separations between particles, inertial ranges, Stokes numbers, and particle drift velocities are considered. We found that the Reynolds number has no effect on the shape evolution of the triangle and tetrahedron provided that the initial distance between the particles is larger than the Kolmogorov length scale.

DOI: 10.1103/PhysRevE.78.016310 PACS number(s): 47.27.tb, 47.27.E−

I. INTRODUCTION

The dispersion of heavy particles is different from that of the carrier fluid as the particles' densities are larger than that of the fluid particles. Such situations are the norm in industrial applications, for example with multiphase processes occurring in combustion. The dispersion process is characterized by both the properties of the heavy particles and the properties of the turbulent fluid that carries the particles, and there are forces acting on the particle because of the relative motion between the particle and the turbulent flow field. These effects cause the particle's velocity to be different from that of the surrounding fluid. Therefore, the trajectory of the heavy particle is different from that of the fluid element. In this paper we deal with isolated particles which do not interact with each other. Furthermore, we make the assumption that their presence does not perturb the turbulent flow. One question that has not received much attention so far concerns the effect of turbulence on the shape and size of sets of heavy particles initially forming an equilateral triangle or tetrahedron. This question has received some answers in the case of diffusion of fluid elements [1,2]. We propose here to generalize that work to particles with inertia in the presence of gravity. The statistical properties of sets of heavy particles are important in many research domains such as the dispersion of plankton on ocean surfaces and the formation of warm clouds, sprays, or particulate pollutants. The importance of following the evolution of n particles in turbulent flows was emphasized in [3] where higher-order structure functions were considered as a way of connecting the scaling properties of turbulence to the spatial structure of the flow. In [4], the statistics of geometrical properties of clusters of three and four material particles were investigated in three-dimensional turbulent flows either by using direct numerical simulation (DNS) at a moderate Reynolds number based on the Taylor microscale ($\mathrm{Re}_\lambda=82$) or by using a simple phenomenological model of Lagrangian kinematics. In [1], the geometrical aspects of Lagrangian dispersion and the shape distortion of small triangles were studied in an experimental two-dimensional turbulent flow with an inverse energy cascade regime with a $k^{-5/3}$ spectrum. The experimental results provided strong evidence that the distortion of the triangle shape depends on its initial size. The dispersion of a three-particle set in a two-dimensional turbulent flow was studied by [5] with the help of kinematic simulation (KS). Two-dimensional KSs were made for direct comparisons with the DNS results and the shape distribution of triangles advected in turbulence was investigated at high Re.

In [6], experimental and numerical studies of the dispersion of particle triplets are carried out in turbulent fluid motion with a free surface. The surface compressibility is found to change the stretching of triangular structures on the surface. The experimental and simulation results there show that the values of the shape factor are below the Gaussian ones. KSs for the time being are limited to incompressible flows (though some attempts are made at understanding the compressibility effect in [7]). More KSs were done in [2], extending the studies of [5]. In particular, the effect of the Re, the initial separation, and the unsteadiness term modeling on three-and four-particle sets advected in an isotropic incompressible three-dimensional turbulent flow was investigated. In the present paper, we further extend the study of [2] to the dispersion of three- and four-*heavy*-particle sets in turbulent flows. In particular, we analyze the effect of the particle's inertia and of gravity on the time evolution of the set shape.

The numerical method we use to generate the turbulent flow, the heavy particle equation of motion, and the parametrization used for characterizing the size and the shape of the heavy particle sets are introduced in Sec. II. The results for the dispersion of three-heavy-particle sets are presented in Sec. III and for the dispersion of four-heavy-particle sets in Sec. IV. We conclude the paper in Sec. V.

II. METHOD

A. Kinematic simulation technique

In order to study turbulent dispersion it may be sufficient to simulate kinematically the turbulent flow in which the particles disperse, without solving explicitly the dynamical equations [8,9]. Simulating turbulence kinematically using

*F.Nicolleau@Sheffield.ac.uk

Fourier modes is called kinematic simulation. This technique has been able to reproduce very well some of the Lagrangian properties [10,11].

The computational simplicity of KS allows one to consider large inertial subranges and Re. KSs are a powerful tool to study the problem of dispersion of heavy particle sets in turbulent flows. With this method, the computational task reduces to the calculation of the trajectory of each particle placed in the turbulent field; each trajectory is, for a given initial condition, a solution of the differential equation

$$\frac{d\mathbf{x}}{dt} = \mathbf{u}_E(\mathbf{x},t), \tag{1}$$

where $\mathbf{u}_E$ is the Eulerian velocity modeled by KS.

The trajectories are independent of each other and calculated using the fourth-order predictor-corrector method (Adams-Bashforth-Moulton) in which the fourth-order Runge-Kutta scheme is used to compute the first three points needed to initiate the Adams-Bashforth method. This kind of computation does not require the storage of a lot of data with very large tables, as with direct numerical simulation.

As in [2,12,13], the three-dimensional KS turbulent velocity field used in this paper is a truncated Fourier series, i.e., the sum of N random Fourier modes:

$$\mathbf{u}(\mathbf{x},t) = \sum_{n=1}^{N} (\mathbf{a}_n \times \hat{\mathbf{k}}_n)\cos(\mathbf{k}_n \cdot \mathbf{x} + \omega_n t) + (\mathbf{b}_n \times \hat{\mathbf{k}}_n)\sin(\mathbf{k}_n \cdot \mathbf{x} + \omega_n t), \tag{2}$$

where N is the number of Fourier modes, and $\hat{\mathbf{k}}_n$ is a random unit vector defined as $\hat{\mathbf{k}}_n = \mathbf{k}_n/|\mathbf{k}_n|$ so that

$$\mathbf{k}_n = |\mathbf{k}_n|\hat{\mathbf{k}}_n = |\mathbf{k}_n| \begin{pmatrix} \sin\theta_n \cos\phi_n \\ \sin\theta_n \sin\phi_n \\ \cos\theta_n \end{pmatrix}, \tag{3}$$

where $\theta_n \in [0,\pi[$ and $\phi_n \in [0,2\pi[$ are picked randomly for each mode and realization so that the random direction for the nth wave mode is independent of the directions of all the other modes. For the sake of completeness we just mention $\omega_n t$, the unsteadiness term. The vectors $\mathbf{a}_n$ and $\mathbf{b}_n$ are random uncorrelated vectors distributed under the constraint that they are normal to $\hat{\mathbf{k}}_n$, and their amplitudes have been chosen according to $|(\mathbf{a}_n \times \hat{\mathbf{k}}_n)|^2 = |(\mathbf{b}_n \times \hat{\mathbf{k}}_n)|^2 = 2E(k)\Delta k_n$. To ensure that the velocity field is incompressible ($\nabla \cdot \mathbf{u} = 0$), the Fourier coefficients are written as $(\mathbf{a}_n \times \hat{\mathbf{k}}_n)$ and $(\mathbf{b}_n \times \hat{\mathbf{k}}_n)$. The value of $|\mathbf{k}_n|$ has to be chosen by discretizing the wave number space into a finite number N of modes. The geometric distribution

$$k_n = k_1 \left(\frac{k_N}{k_1}\right)^{(n-1)/(N-1)} \tag{4}$$

is chosen because it leads to equally spaced energy shells for $\ln(k)$. The wave number increment Δk_n is defined as follows:

$$\Delta k_1 = \frac{(k_2 - k_1)}{2} \quad \text{for } n = 1,$$

$$\Delta k_n = \frac{(k_{n+1} - k_{n-1})}{2} \quad \text{for } n \in [2, k_{N-1}],$$

$$\Delta k_N = \frac{(k_N - k_{N-1})}{2} \quad \text{for } n = k_N. \tag{5}$$

In this study, we use an energy spectrum characterized by a power law with an exponent of $-5/3$ which does not change with time (nondecaying turbulence):

$$E(k_n) = C_k \varepsilon^{2/3} k_n^{-5/3} \quad \text{for } k_1 \le k_n \le k_N, \tag{6}$$

where C_k is the Kolmogorov constant ($C_k = 1.5$) and ε the dissipation rate of energy per unit mass. Outside the range $[k_1, k_N]$, $E(k) = 0$ and the total kinetic energy E is obtained by integrating the energy spectrum over the total range of wave numbers,

$$E = \int_{k_1}^{k_N} E(k)dk. \tag{7}$$

The rms of the turbulent velocity fluctuation is

$$u' = \sqrt{\frac{2}{3}\int_{k_1}^{k_N} E(k_n)dk}. \tag{8}$$

The integral length scale of the isotropic turbulence is defined as follows:

$$L = \frac{3\pi}{4} \frac{\int_{k_1}^{k_N} k^{-1}E(k_n)dk}{\int_{k_1}^{k_N} E(k_n)dk}. \tag{9}$$

The Kolmogorov length scale is defined as $\eta = 2\pi/k_N$. The ratio between the integral and Kolmogorov length scales is $L/\eta = k_N/k_1$, which is used to determine the inertial range and the associated Re: $\mathrm{Re} = (L/\eta)^{4/3} = (k_N/k_1)^{4/3}$. The pulsation ω_n in (2) determines the unsteadiness that can be associated with the nth wave mode. It has been shown in [10] that in three-dimensional isotropic KSs for two-particle diffusion, most of the statistical properties are insensitive to the unsteadiness parameter's value. In accordance with these results we have not added any unsteadiness term ($\omega_n = 0$) to our KS simulations.

One of the important time scales existing in the turbulent flow is the eddy turnover time, which corresponds to the integral length scale L. The turnover time is defined as $t_d = L/u'$. The other important time scale is the Kolmogorov time scale, which corresponds to the Kolmogorov length scale; it is defined as $t_\eta = t_d(\eta/L)^{2/3}$. The time step used for the KS is determined by tracking the motion of fluid elements down to the smallest scales; it must be smaller than both the smallest eddy turnover time and the time that a typical fluid particle would take, on average, to move by a Kolmogorov length scale. According to [14], a time step equal to $0.1t_\eta$ is small enough to ensure that the results are independent of the time step.

TABLE I. Different cases for three- and four-heavy-particle sets, introducing the effect of inertia.

Case	Δ_0/η	St	St_η	γ	k_N/k_1	η	u'	t_d	Case	Δ_0/η	St	St_η	γ	k_N/k_1	η	u'	t_d
A1	0.09	1	32.47	0	185	3.39×10^{-2}	1	1	K1	16	1	32.47	0	185	3.39×10^{-2}	1	1
B1	0.25	0.2	6.49	0	185	3.39×10^{-2}	1	1	L1	16	2	64.93	0	185	3.39×10^{-2}	1	1
C1	0.25	0.4	12.98	0	185	3.39×10^{-2}	1	1	M1	92.5	0.2	6.49	0	185	3.39×10^{-2}	1	1
D1	0.25	0.8	25.97	0	185	3.39×10^{-2}	1	1	N1	92.5	1	32.47	0	185	3.39×10^{-2}	1	1
E1	0.25	1	32.47	0	185	3.39×10^{-2}	1	1	O1	0.5	1	99.95	0	1000	6.28×10^{-3}	1	1
F1	6	1	32.47	0	185	3.39×10^{-2}	1	1	P1	32	1	99.95	0	1000	6.28×10^{-3}	1	1
G1	16	0.2	6.49	0	185	3.39×10^{-2}	1	1	Q1	500	1	99.95	0	1000	6.28×10^{-3}	1	1
H1	16	0.4	12.98	0	185	3.39×10^{-2}	1	1	R1	1	1	158.66	0	2000	3.14×10^{-3}	1	1
I1	16	0.6	19.47	0	185	3.39×10^{-2}	1	1	S1	64	1	158.66	0	2000	3.14×10^{-3}	1	1
J1	16	0.8	25.97	0	185	3.39×10^{-2}	1	1	T1	1000	1	158.66	0	2000	3.14×10^{-3}	1	1

B. Heavy particle equation of motion

The complete equation of motion for heavy particles is still the subject of current research. Depending on the degree of simplification, it can involve different forces acting on the particle. These can be, for example, the lift force due to the nonuniform distribution of the flow field around the particle, the drag force due to the relative motion between the particle itself and the surrounding fluid elements, the gravity force, the buoyancy force, and the force due to the unsteadiness of the flow.

Let us consider a heavy particle with its center positioned at $\mathbf{x}_p(t)$ at time t; it moves with a velocity $\mathbf{V}_p(t)$ in a surrounding flow of velocity $\mathbf{u}(\mathbf{x}_p,t)$. The equation of motion of a heavy particle derived in [15] can be simplified to the form used in [16,17], which reduces the computational cost. In a frame of reference moving with the center of the particle, the particle acceleration can be described as follows:

$$m_p \frac{d\mathbf{V}_p}{dt} = m_p\mathbf{g} - 6\pi a\mu[\mathbf{V}_p(t) - \mathbf{u}(\mathbf{x}_p(t),t)], \qquad (10)$$

where m_p is the mass of the particle, $\mathbf{g}$ the gravity, a the spherical particle's radius, and μ the dynamic viscosity of the fluid. Another form of Eq. (10) is

$$\frac{d\mathbf{V}_p}{dt} = \frac{\mathbf{u}(\mathbf{x}_p(t),t) - \mathbf{V}_p(t) + \mathbf{V}_d}{\tau_a}, \qquad (11)$$

where $\tau_a = m_p/6\pi a\mu$ is the particle's aerodynamic response time and $V_d = \tau_a g$ the particle's terminal fall velocity or drift velocity. Because the dispersion is controlled by the large-scale eddies, the parameters V_d and τ_a can be rescaled by the turbulence rms velocity u' and the largest eddy turnover time t_d; we therefore introduce the two usual dimensionless parameters as follows.

(1) The Stokes number $\mathrm{St} = \tau_a/t_d$, which expresses the ratio between the particle's response time and the turbulence characteristic time. Based on the largest eddy, it measures the relative importance of the particle inertia. In the limiting case St=0, the particles with inertia recover the motion of the fluid particles, whereas for $\mathrm{St}\to\infty$ the particles become less and less influenced by the surrounding velocity field. It is possible to define another Stokes number based on the Kolmogorov time scale as $\mathrm{St}_\eta = \tau_a/t_\eta$. For the sake of completeness we also report that number in Tables I and II. The relation between these two numbers is $\mathrm{St}_\eta = \mathrm{St}(L/\eta)^{2/3}$, so there are some cases where we varied the ratio (L/η) where St is constant whereas St_η is not. The choice of taking St as our

TABLE II. Different cases for three- and four-heavy-particle sets with gravity effect.

Case	Δ_0/η	St	St_η	γ	k_N/k_1	η	u'	t_d	Case	Δ_0/η	St	St_η	γ	k_N/k_1	η	u'	t_d
A2	0.09	0.02	0.649	1	185	3.39×10^{-2}	0.44	2.23	M2	0.5	0.02	1.999	1	1000	6.28×10^{-3}	0.44	2.23
B2	0.25	0.02	0.649	0.2	185	3.39×10^{-2}	1	1	N2	32	0.02	1.999	0.2	1000	6.28×10^{-3}	1	1
C2	0.25	0.02	0.649	0.4	185	3.39×10^{-2}	0.698	1.41	O2	32	0.02	1.999	1	1000	6.28×10^{-3}	0.44	2.23
D2	0.25	0.02	0.649	1	185	3.39×10^{-2}	0.44	2.23	P2	500	0.02	1.999	0.2	1000	6.28×10^{-3}	1	1
E2	0.25	0.02	0.649	2	185	3.39×10^{-2}	0.313	3.146	Q2	500	0.02	1.999	0.8	1000	6.28×10^{-3}	0.485	2.02
F2	6	0.02	0.649	0.2	185	3.39×10^{-2}	1	0.2	R2	500	0.02	1.999	1	1000	6.28×10^{-3}	0.44	2.23
G2	6	0.02	0.649	1	185	3.39×10^{-2}	1	0.2	S2	500	0.02	1.999	2	1000	6.28×10^{-3}	0.313	3.146
H2	92.5	0.02	0.649	0.2	185	3.39×10^{-2}	1	0.2	T2	1	0.02	3.173	1	2000	3.14×10^{-3}	0.44	2.23
I2	92.5	0.02	0.649	0.4	185	3.39×10^{-2}	0.698	1.41	U2	64	0.02	3.173	0.2	2000	3.14×10^{-3}	1	1
J2	92.5	0.02	0.649	0.8	185	3.39×10^{-2}	0.485	2.02	V2	64	0.02	3.173	1	2000	3.14×10^{-3}	0.44	2.23
K2	92.5	0.02	0.649	1	185	3.39×10^{-2}	0.44	2.23	W2	1000	0.02	3.173	0.2	2000	3.14×10^{-3}	1	1
L2	92.5	0.02	0.649	2	185	3.39×10^{-2}	0.313	3.146	X2	1000	0.02	3.173	1	2000	3.14×10^{-3}	0.44	2.23

reference is dictated by previous results showing that in most situations the relevant ratio is L/Δ_0. That is, provided that $\Delta_0 > \eta$, η (or Re) does not matter [2].

(2) The drift velocity parameter $\gamma = V_d/u'$, which is the ratio between the particle's drift velocity and the turbulence rms velocity.

For each of our simulations, the statistics were obtained by taking an ensemble average over 4000 realizations of the flow. We tried different numbers of realizations and checked that statistics and the different trends we observe do not change after 3000 realizations. All simulations reported here were performed using 200 Fourier modes ($N=200$).

C. Heavy particle set parametrization

In this section, three- and four-heavy-particle set parametrizations are introduced in order to characterize the size and shape distortion in these sets.

1. Three-particle set

Three particles form a triangle with vertices located at X_1, X_2, and X_3 (see, e.g., Fig. 1 in [2]). The initial positions of the particles are chosen randomly in each realization. In practice, the initial position of the first particle is chosen randomly, then the other particles' positions are calculated relative to the first particle. The initial separation between any two particles is set to $\Delta_0 = n\eta$ where n varies from 0.25 to 1000 depending on the choice of the inertial subrange, and for more randomness the initial position arrangement is rotated by a random angle in each realization. The evolution of the size and shape of the three-particle set is described using Euler's parametrizations as in [1,4].

For the size variation, three reduced coordinates are defined as follows: $\boldsymbol{\rho}_0 = (\mathbf{X}_1 + \mathbf{X}_2 + \mathbf{X}_3)/2$, $\boldsymbol{\rho}_1 = (\mathbf{X}_2 - \mathbf{X}_1)/\sqrt{2}$, and $\boldsymbol{\rho}_2 = (2\mathbf{X}_3 - \mathbf{X}_2 - \mathbf{X}_1)/\sqrt{6}$. Because of the homogeneity of the velocity field and initial distributions of the particles, the Lagrangian statistics are independent of the center of mass ρ_0. The radius of gyration, which is used to characterize the overall size of the triangle, is defined as $R^2 = \Sigma_{i=1}^2 \rho_i^2 = \rho_1^2 + \rho_2^2 = (\mathbf{r}_{12}^2 + \mathbf{r}_{23}^2 + \mathbf{r}_{31}^2)/3$, where $\mathbf{r}_{ij} = \mathbf{X}_j - \mathbf{X}_i$ is the triangle side length. The triangle area is defined as $A = |\rho_1 \times \rho_2|$.

For the shape variation as in [4], the "moment-of-inertia-like" tensor is introduced as follows:

$$g^{ab} = \sum_{i=1}^{2} \rho_i^a \rho_i^b, \tag{12}$$

where ρ_i^a is the a component of the vector ρ_i. For three-dimensional velocity fields, there are three eigenvalues g_i of the moment of inertia matrix $I = \rho\rho^T$, where $g_1 \geq g_2 \geq g_3$, that describe the spatial extension of the triangle in the three-dimensional turbulence. The triangle continuously experiences dilatation, rotation, and translation during its evolution in the turbulent flow. Its shape varies continuously; this evolution can be quantified with I_2, which is defined as the ratio between g_2 and R^2,

$$I_2 = \frac{g_2}{R^2}. \tag{13}$$

It can be shown that $0 \leq I_2 \leq 1/2$ an equilateral triangle corresponds to $I_2 = 1/2$; smaller values of I_2 correspond to more elongated triangles. The other method to describe the shape of the triangle is to use the parameters W and χ [1] which are defined as follows:

$$W = \frac{2|\rho_1 \times \rho_2|}{R^2} \quad (W \in [0,1]), \tag{14}$$

$$\chi = \frac{1}{2} \arctan\left(\frac{2\rho_1 \cdot \rho_2}{\rho_2^2 - \rho_1^2}\right) \quad \left(0 \leq \chi \leq \frac{\pi}{6}\right). \tag{15}$$

I_2 can be related to the parameter W as $I_2 = (1 - \sqrt{1 - W^2})/2$, so we will present here only the shape factor W as a measure for the shape variation for the three-heavy-particle set. The value $W=0$ indicates that the three points are aligned, whereas the value $W=1$ corresponds to an equilateral triangle; small values of χ indicate that the separation between two particles (e.g., 1 and 2) is much smaller than their separation from the third one.

2. Four-particle set

As for three-particle sets and using Euler's parametrizations as in [4,18], the tetrahedron's vertices are located at X_1, X_2, X_3, and X_4 (see, e.g., Fig. 2 in [2]). For the size variation, a set of four reduced vectors ρ_i is used as follows: $\rho_0 = (\mathbf{X}_1 + \mathbf{X}_2 + \mathbf{X}_3 + \mathbf{X}_4)/2$, $\rho_1 = (\mathbf{X}_2 - \mathbf{X}_1)/\sqrt{2}$, $\rho_2 = (2\mathbf{X}_3 - \mathbf{X}_2 - \mathbf{X}_1)/\sqrt{6}$, and $\rho_3 = (3\mathbf{X}_4 - \mathbf{X}_3 - \mathbf{X}_2 - \mathbf{X}_1)/\sqrt{12}$. The radius of gyration, which is used to characterize the global size of the tetrahedron, represents the spatial extent of the four-particle set (or tetrahedron); it can be defined as $R^2 = \Sigma \rho_i^2 = \rho_1^2 + \rho_2^2 + \rho_3^2 = (\mathbf{r}_{12}^2 + \mathbf{r}_{23}^2 + \mathbf{r}_{34}^2 + \mathbf{r}_{41}^2)/4$, where $\mathbf{r}_{ij} = |\mathbf{X}_j - \mathbf{X}_i|$ is the tetrahedron side length. The tetrahedron's volume, which can give the information about three-dimensional structure, is defined as $V = |\det(\rho_1, \rho_2, \rho_3)|$.

For the shape variation, the moment-of-inertia-like tensor is used to characterize the shape of the four-particle set; there are three eigenvalues g_1, g_2, and g_3 that describe the spatial extension of the tetrahedron in the three-dimensional turbulence. Here, we choose the shape factor I_2^{th} as a measure for the shape variation for the four-heavy-particle set, where "th" stands for the tetrahedron case, in order to introduce a different notation from that for three particles in the previous section. $g_1 = g_2 = g_3$ corresponds to an isotropic object, $g_3 = 0$ corresponds to four points that are coplanar, and $g_2 = g_3$ corresponds to a collinear configuration.

3. Evolution of heavy particle sets in turbulent flow

The equation of motion (11) is integrated over 4000 realizations of the flow. This number of realizations is enough to give smooth curves except perhaps for $\langle\chi\rangle$, which by its definition requires more numerical precision. However, no significant difference was observed between 3000 or 4000 realizations. The numerical error in the computation of $\langle\chi\rangle$ can be estimated from the oscillations we observed for $t/t_d > 10$, which are below 5%.

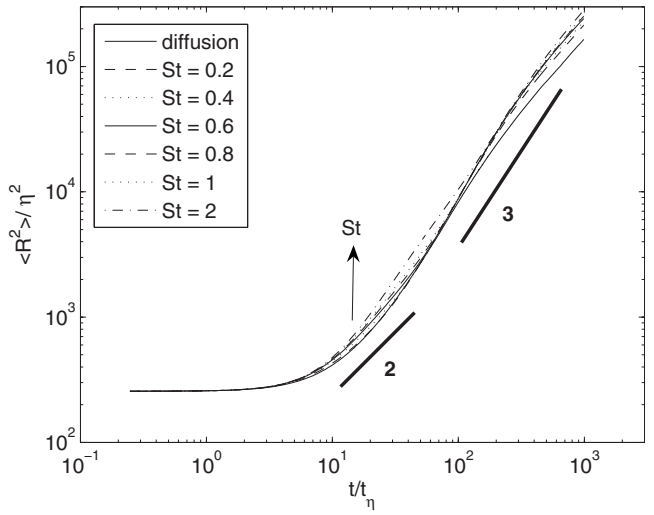

FIG. 1. Triangle's size normalized by the Kolmogorov length scale $\langle R^2\rangle/\eta^2$ as a function of t/t_η (cases G1, H1, I1, J1, K1, and L1 in Table I).

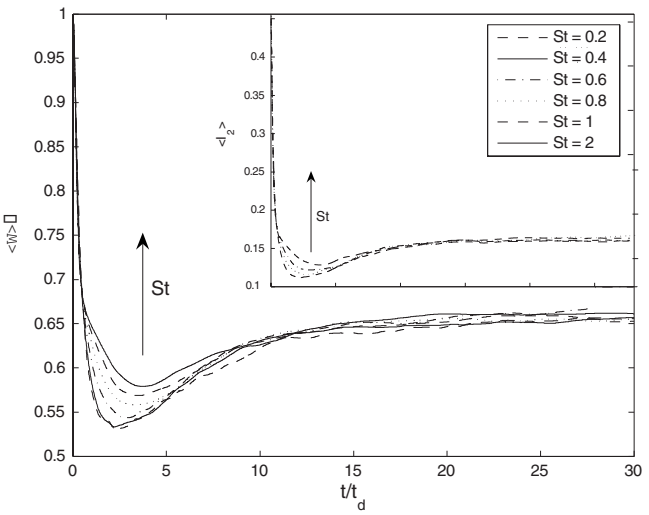

FIG. 2. Time evolution of the triangle shape factor $\langle W\rangle$ for particles with inertia only, for cases G1, H1, I1, J1, K1, and L1 in Table I. In the inset, time evolution of the triangle shape factor $\langle I_2\rangle$.

The initial velocity of the heavy particle is set to be the same as that of the fluid element, $\mathbf{V}_p(t=0)=\mathbf{u}(\mathbf{x}_p(t=0),0)+\mathbf{V}_d$. The time step is chosen smaller than the Kolmogorov time scale. The particle time constant τ_a is always chosen larger than the smallest time scale of the turbulent flow (t_η). Runs have been made for $k_N/k_1=185$, 1000, and 2000; in order to study the effect of Re. In all cases studied here the unsteadiness term ω_n is equal to 0. The values of St are set to 0.02, 0.2, 0.4, 0.6, 0.8, 1, and 2, and the values of the particle drift velocity are set to 0.2, 0.4, 0.8, 1, and 2. All the run parameters are tabulated in Table I for the study of the inertia effect and in Table II for the study of the gravity effect.

III. RESULTS FOR THREE-HEAVY-PARTICLE SETS

In this section, we study the effect of particle inertia and of gravity on three-heavy-particle sets for different initial separations and different inertial ranges. The calculations are made for different particle inertias with and without gravity (different values of γ).

A. Effect of particle inertia on a three-heavy-particle set

In this section, we limit our study to the effect of the particle inertia alone. We change St, but remove any effect of gravity by setting $\gamma=0$, and study the dispersion of three-heavy-particle triangles, initially equilateral, moving in an isotropic turbulence. In the absence of gravity, the particle dispersion is isotropic; the particles leave the fluid particle path only because of the inertia effect. The triangle size is monitored as a function of time by computing the evolution of $\langle R^2\rangle^{1/2}$, where R is the triangle's radius of gyration. The changes in the triangle shape are monitored by using the parameters $\langle W\rangle$, $\langle I_2\rangle$, and $\langle\chi\rangle$ as functions of time.

1. Effect of variation of St for a given initial separation

The effect of particle inertia on the dispersion of three-particle sets in an isotropic turbulent flow is studied for a given initial separation $\Delta_0/\eta=16$, and a zero drift velocity. The evolution of the size and shape of an initially equilateral triangle that is immersed in an isotropic turbulent flow are presented in Figs. 1–3.

The effect of St on the triangle's size can be observed in Fig. 1, where the three-heavy-particle set size $\langle R^2\rangle/\eta^2$ is plotted as a function of time and for the sake of comparison the same result for three-particle diffusion is also plotted. In Fig. 1, St is varied from 0.2 to 2.

It was shown [13] that when St increases, the time needed to see the beginning of a Richardson regime is also increased. Before the Richardson regime starts, the particle separation is small; the particles tend to move following straight lines. In this regime $\langle R^2\rangle$ follows the form of a power law t^2 [13],

$$\langle R^2\rangle=\Delta_0^2+(\Delta\mathbf{V}_0)^2t^2, \tag{16}$$

where ΔV_0 is the particles' velocity difference at $t=0$ and Δ_0 is the initial separation between the triangle vertices. This

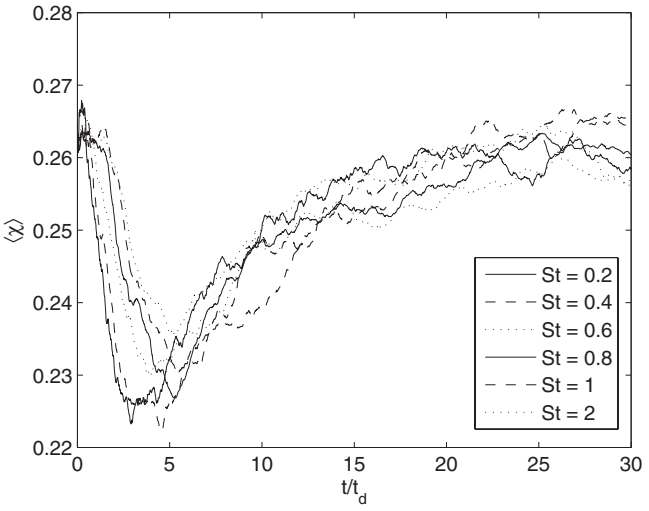

FIG. 3. Time evolution of the triangle shape factor $\langle\chi\rangle$ for particle with inertia for cases G1, H1, I1, J1, K1, and L1 in Table I.

TABLE III. Different values for the shape factors for three-particle sets.

Coefficient	KS with inertia	KS without inertia [2]	Experimental, two dimensions, without inertia [1]	Gaussian values
$\langle W\rangle_{\text{asy}}$	0.65	0.66	0.5	0.5
$\langle I_2\rangle_{\text{asy}}$	0.165	0.16	0.11	0.107
$\langle \chi\rangle_{\text{asy}}$	0.26	0.26	0.25	0.262

initial regime prevents the Richardson regime from occurring, and lasts longer when St increases. This is because the larger the particles' inertia the longer they remember their initial state. As the time is increased and reaches the relaxation time for the particle, τ_a, turbulence comes into play, producing the Richardson regime where the particles may follow the celebrated t^3 power law [13].

The effect of St on the triangle's shape can be seen in Figs. 2 and 3. The local minimum of the shape factors ($\langle W\rangle$, $\langle I_2\rangle$, and $\langle \chi\rangle$) measures the departure from the asymptotic value; this departure decreases when St increases. The small-St sets are experiencing high distortion in shape and the shape factors rapidly decrease to a local minimum value before reaching their asymptotic value. When St is increased, the shape factors reach their asymptotic values, which have been observed not to depend on St or the initial separations, at $t/t_d=15$, directly without passing through a minimum value. These asymptotic values are reported in Table III and compared with [1] whose data correspond to DNS and [2] whose data were obtained from KS. Our results are close enough to those of [2] for the conclusion that inertia has no effect on the asymptotic values for the dispersion of three-heavy-particle sets for St in the range $0.2 \leq \text{St} \leq 2$.

As shown in Fig. 4, the local-minimum departure from the asymptotic value of the shape factors $\langle W\rangle$ can be related to St as follows:

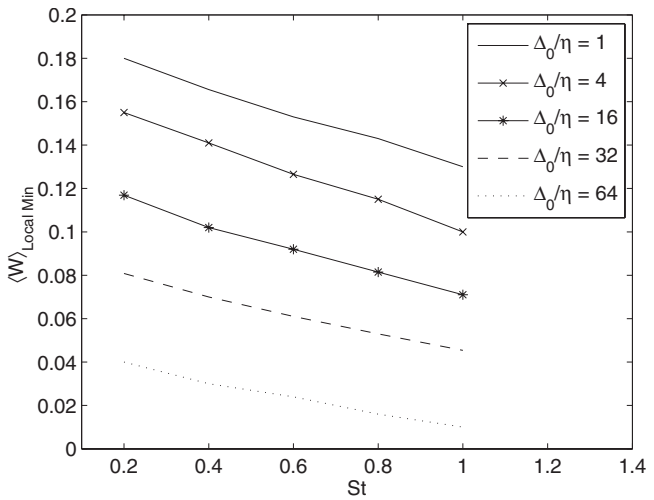

FIG. 4. Local-minimum value of the triangle shape factor $\langle W\rangle$ as a function of St for $k_N/k_1=185$.

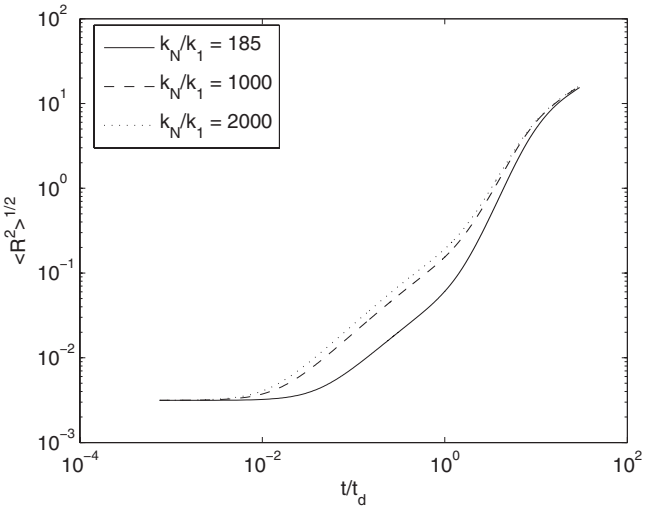

FIG. 5. Time evolution of the triangle size for the initial separation $\Delta_0/L_1=0.0005$ for particles with inertia (for cases A1, O1, and R1 in Table I).

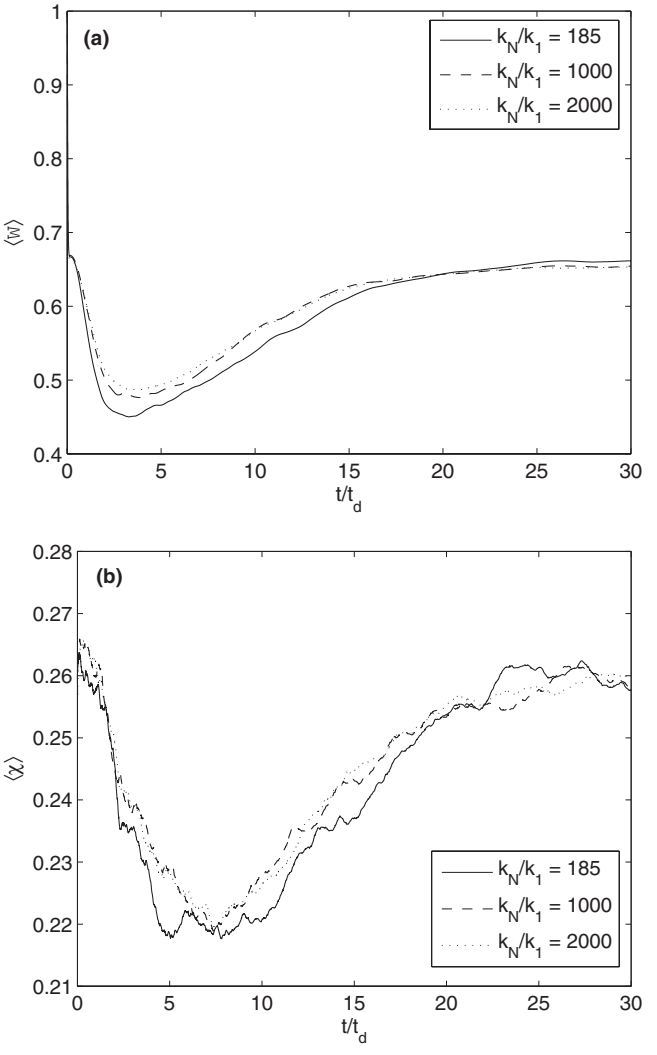

FIG. 6. Time evolution of the triangle shape factors (a) $\langle W\rangle$ and (b) $\langle \chi\rangle$, for the initial separation $\Delta_0/L_1=0.0005$ (for cases A1, O1, and R1 in Table I).

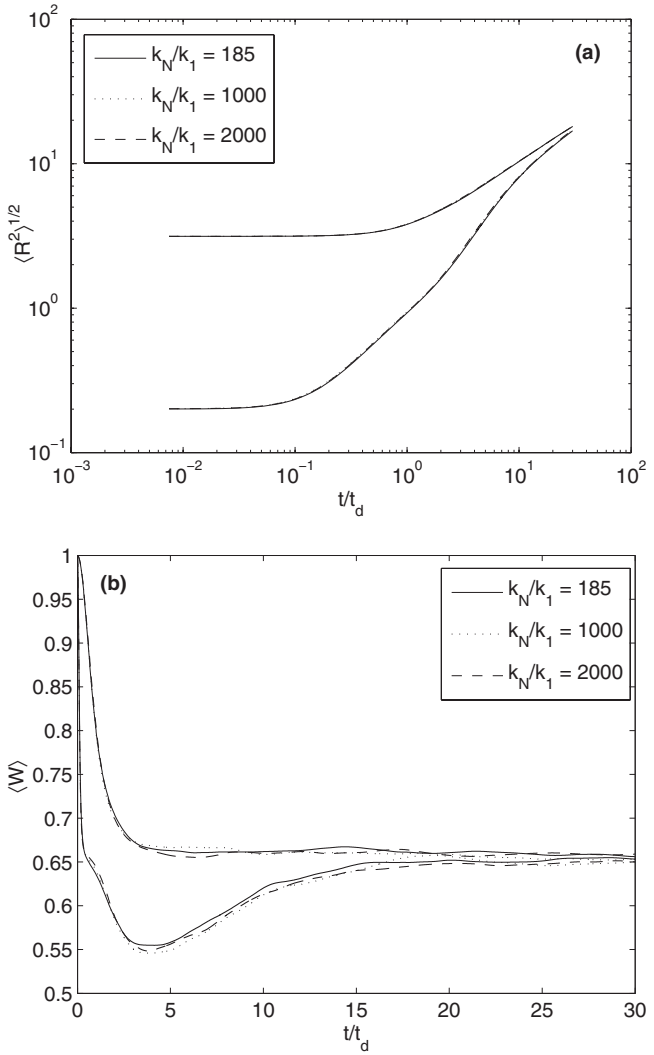

FIG. 7. Time evolution of (a) the triangle size and (b) the triangle shape factor $\langle W \rangle$ for two initial separations, top $\Delta_0/L_1=0.5$nd bottom $\Delta_0/L_1=0.032$, for different Re (cases F1, N1, P1, Q1, S1, and T1 in Table I).

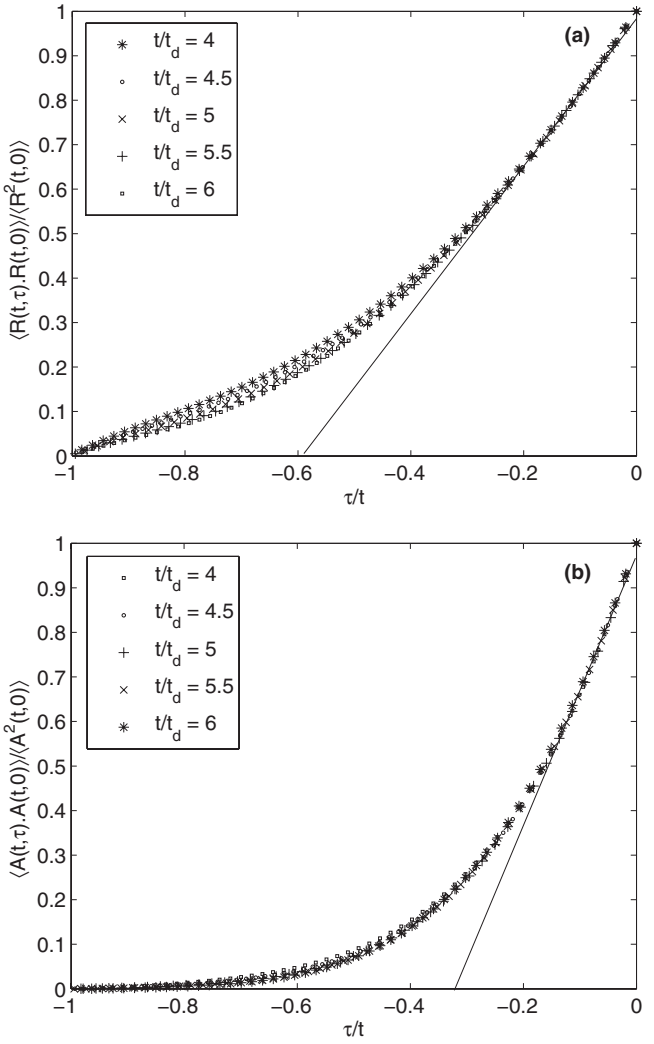

FIG. 8. Lagrangian autocorrelation function of (a) the normalized triangle size and (b) the normalized triangle area, for different times $4 \leq t/t_d \leq 6$ and St=1 (case E1 in Table I).

$$\langle W \rangle_{\min} = A\ \mathrm{St} + B, \tag{17}$$

where A and B are functions of the initial separation Δ_0/η only. Furthermore, A and B can be found as functions of the initial separation:

$$A = 0.0065 \ln\frac{\Delta_0}{\eta} - 0.0685, \tag{18}$$

$$B = -0.0341 \ln\frac{\Delta_0}{\eta} + 0.2045; \tag{19}$$

then

$$\langle W \rangle_{\min} = [0.0065 \ln(\Delta_0/\eta) - 0.0685]\mathrm{St} + [-0.0341 \ln(\Delta_0/\eta) + 0.2045]. \tag{20}$$

This equation contains the effect of St and of the initial separation on the shape factor of the three-heavy-particle sets.

2. Effect of Re for particles with inertia

Figures 5–7 show the results for different Re (from $k_N/k_1=185$ to 2000) at a given St, St=1, and for different initial separations either smaller or larger than the Kolmogorov length scale. The time evolution of the triangle's size and shape factors for different initial separations are shown in Figs. 5 and 6 for $\Delta_0/L_1=0.0005$, which corresponds to a case where $\Delta < \eta$, and in Fig. 7 for $\Delta_0/L_1=0.032$ and $\Delta_0/L_1=0.5$, which are cases where $\Delta > \eta$.

All the curves of $\langle R^2 \rangle^{1/2}$ and $\langle W \rangle$ for a constant value of $\Delta_0/L_1=0.032$ and $\Delta_0/L_1=0.5$, shown in Fig. 7, approximately collapse. This result was obtained in the case of diffusion in [2]. However, for $\Delta_0/L_1=0.0005$, where the initial separation between the heavy particles is smaller than the Kolmogorov length scale, the curves of $\langle R^2 \rangle^{1/2}$ and $\langle W \rangle$ do not collapse (as shown in Figs. 5 and 6).

We extend the results in [2] to three-heavy-particle dispersion for St in the range $0.2 \leq \mathrm{St} \leq 1$ at a zero drift velocity and for inertial range $185 \leq k_N/k_1 \leq 2000$. However, we limit this result to initial separations above the Kolmogorov length

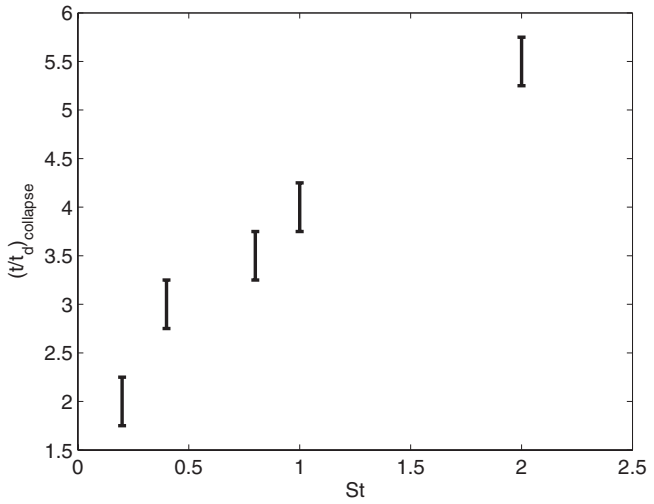

FIG. 9. Relation between St and the normalized time at which the Lagrangian correlation functions collapse.

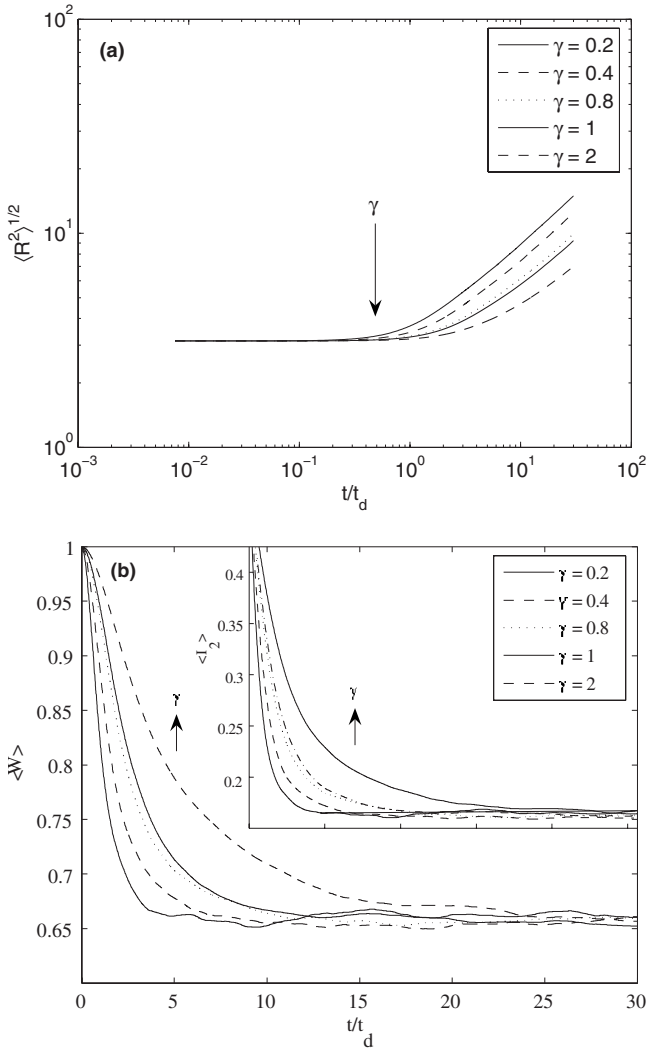

FIG. 10. Time evolution of (a) the triangle size and (b) the triangle shape factor $\langle W \rangle$ ($\langle I_2 \rangle$ in the inset), for particles with a drift velocity for St=0.02 (for cases H2, I2, J2, K2, and L2 in Table II) of γ=0.2, 0.4, 0.8, 1, and 2.

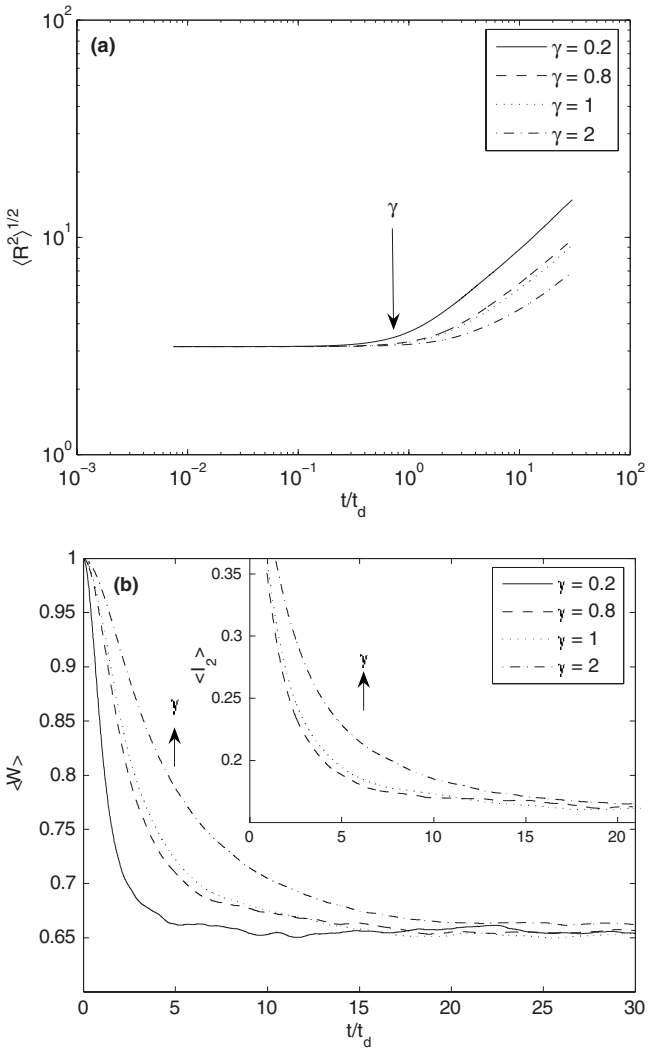

FIG. 11. Time evolution of (a) the triangle size and (b) the triangle shape factor $\langle W \rangle$ ($\langle I_2 \rangle$ in the inset), for particles with a drift velocity for St=0.02 (for cases P2, Q2, R2, and S2 in Table II) of γ=0.2, 0.8, 1, and 2.

scale only. We also find that as the initial triangle size increases the shape distortion becomes weaker. When the initial triangle size becomes comparable to the largest length scale L_1 ($\Delta_0 \approx 0.5L_1$), Fig. 7, we find that the parameters describing the shape change decrease from their initial values to their asymptotic values directly, without passing through a minimum value, in contrast to what is seen for smaller initial triangle sizes ($\Delta_0 \ll 0.5L_1$).

3. The Lagrangian autocorrelation function in the presence of a particle with inertia

In this section, we use KS to produce the Lagrangian autocorrelation function of the three-heavy-particle set to measure the effect of particle inertia on the correlation function for the triangle area A. The normalized Lagrangian autocorrelation functions for the three-heavy-particle set area and size are calculated as follows:

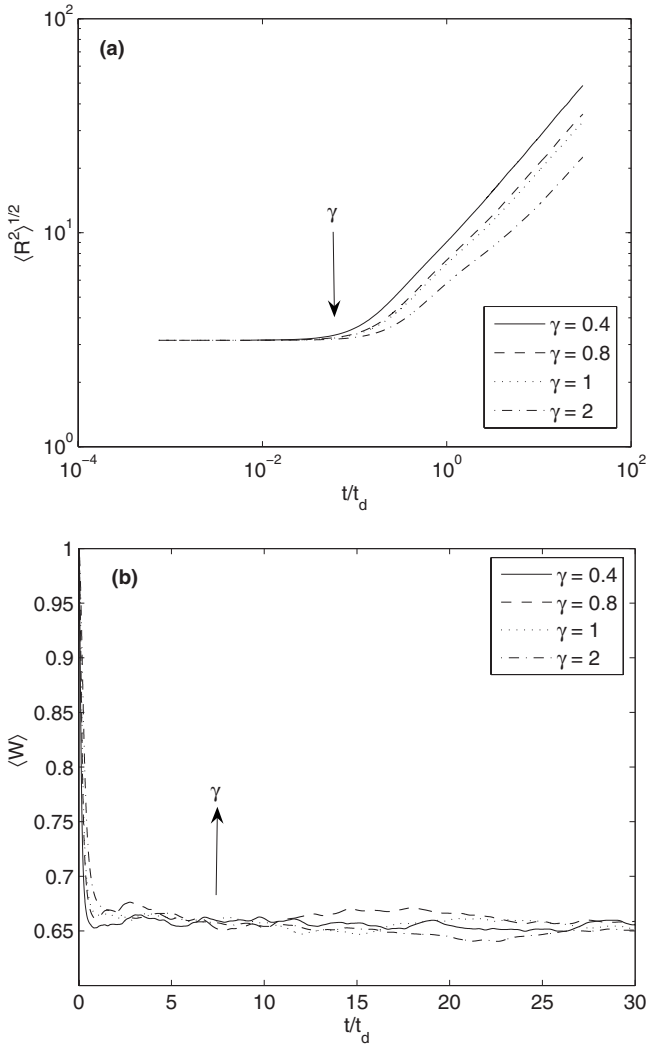

FIG. 12. Time evolution of (a) the triangle size and (b) the triangle shape factor $\langle W \rangle$, for particles with a drift velocity for St $=2$ (cases H2, I2, J2, K2, and L2 in Table II) of γ=0.4, 0.8, 1, and 2.

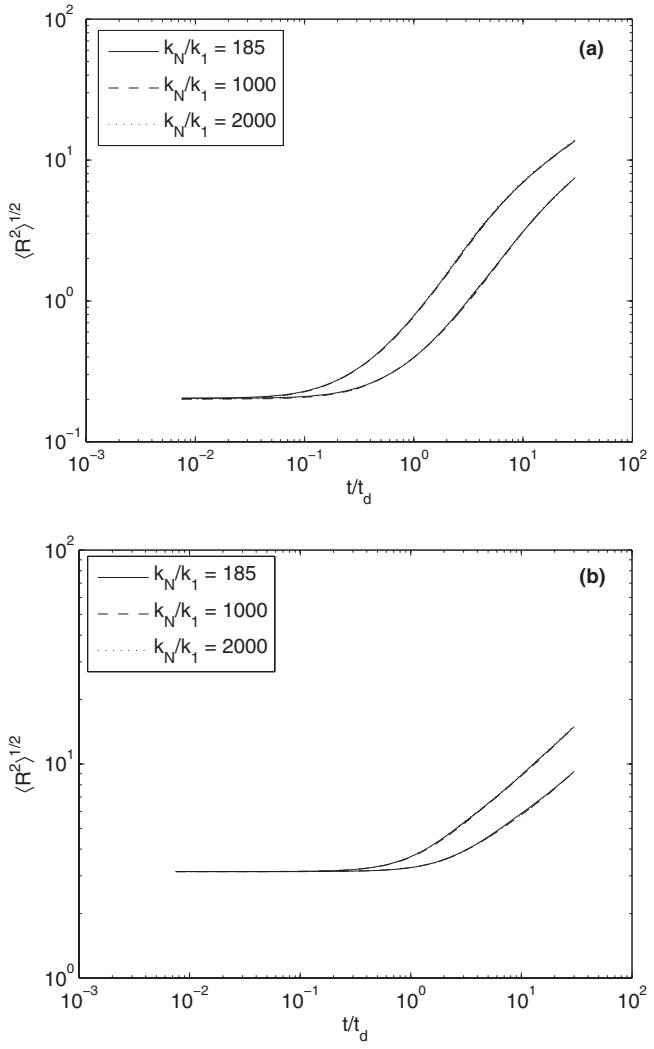

FIG. 13. Time evolution of the triangle size for St=0.02: (a) Δ_0/L_1=0.032, top curves γ=0.2 (cases F2, N2, and U2 in Table II), bottom curves γ=1 (cases G2, O2, and V2 in Table II); (b) Δ_0/L_1 =0.5, top curves γ=0.2 (cases H2, P2, and W2 in Table II), bottom curves γ=1 (cases K2, R2, and X2 in Table II).

$$R(t,\tau) = \langle A(t+\tau)A(t)\rangle / \langle A^2(t)\rangle \tag{21}$$

and plotted as functions of the normalized time lag in order to find the time after which the normalized curves collapse. Figure 8 shows that this has happened after $t/t_d \geq 4$.

From Fig. 8, the correlation time for the triangle size is found to be C_S=0.58 at a St of 1 for a three-heavy-particle set, which indicated that the particles in the set remember about 0.58 of their history; this value slightly differs from the one obtained by [2] where it was C_S=0.65 for a three-particle set of the fluid element case. The correlation time for the triangle area at the same St is found to be C_A=0.32, which indicates that the set remembers about 0.32 of its history. This can be explained as the area order of magnitude is the square of the triangle size, so one would expect two-dimensional information to be lost faster than one dimensional. More precisely, Fig. 9 shows the time t/t_d after which the curves for the area correlation collapse, as a function of St.

This time is clearly an increasing function of St. So with more inertia the triangle takes longer to forget its initial configuration. In other words, at the time at which the curves collapse, that is, when the particles in the set have forgotten their initial separations, the Richardson regime can start, and, as observed before, we can conclude that this regime is delayed as St increases. We can conclude that these two correlation times do not depend significantly on the inertia in the range $0 < \mathrm{St} \leq 2$.

B. Effect of particle gravity on a three-heavy-particle set

In this section, we study the effect of gravity on the dispersion of three heavy particles initially released on an equilateral triangle. In practice, we change the drift velocity parameter γ by changing the turbulent flow parameters and St is set to St=0.02 and 2.

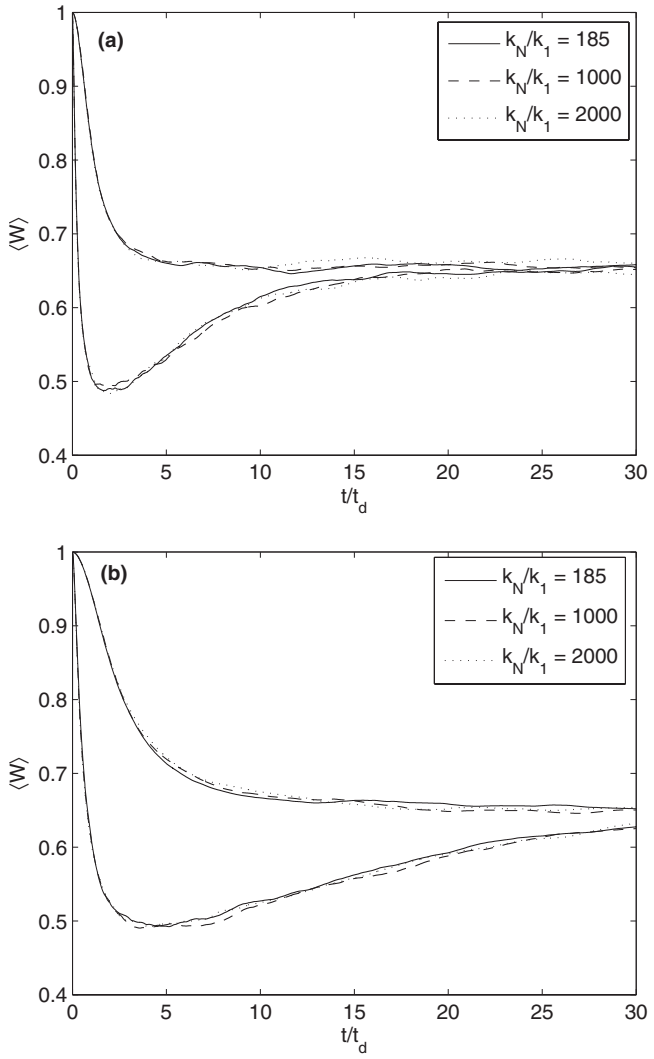

FIG. 14. Time evolution of the triangle shape factor $\langle W \rangle$ for St=0.02: (a) γ=0.2, top curves Δ_0/L_1=0.5 (cases H2, P2, and W2 in Table II), bottom curves Δ_0/L_1=0.032 (cases F2, N2, and U2 in Table II); (b) γ=1, top curves Δ_0/L_1=0.5 (cases K2, R2, and X2 in Table II), bottom curves Δ_0/L_1=0.032 (cases G2, O2, and V2 in Table II).

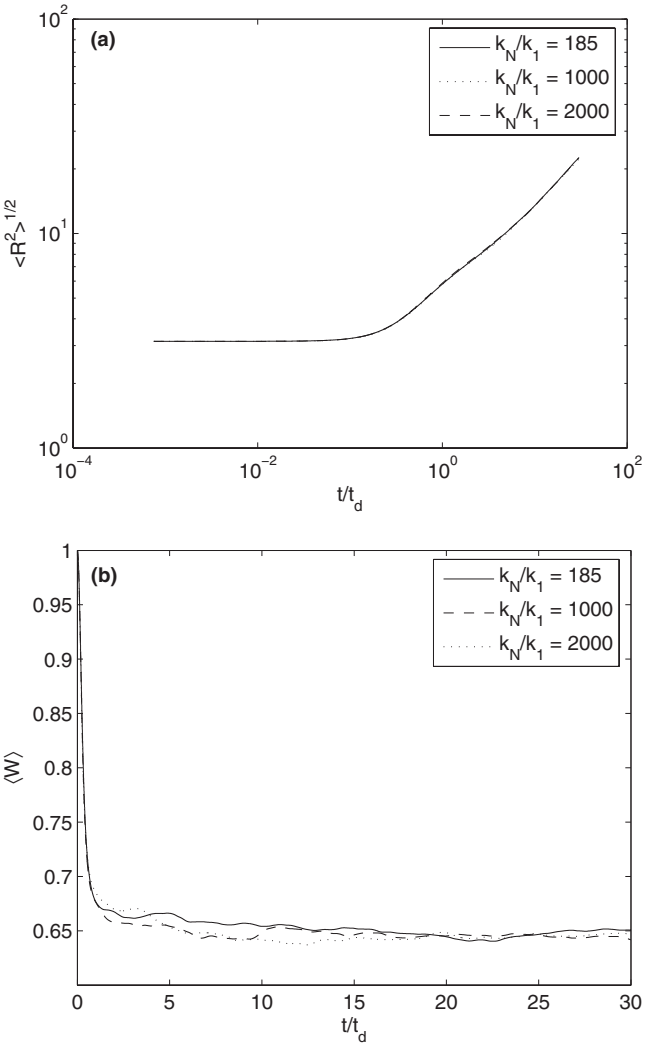

FIG. 15. Time evolution of (a) the triangle size and (b) the triangle shape factor $\langle W \rangle$ for Δ_0/L_1=0.5, γ=0.2, and St=2 (cases H2, P2, and W2 in Table II).

1. Effect of varying the particle drift velocity for a given initial separation

The evolution of the size and shape of an initially equilateral triangle immersed in isotropic turbulence is studied when the drift velocity is varied, $0.2 \leq \gamma \leq 2$, at two particle inertias, St=0.02 and 2, and for a fixed initial separation Δ_0/η. The triangle's size and shape factors are plotted as functions of the time, normalized by the largest eddy turnover time, for the particle drift velocities $0.2 \leq \gamma \leq 2$ and St =0.02, in Fig. 10 (initial separation Δ_0/η=92.5) and Fig. 11 (initial separation Δ_0/η=500). In Fig. 13 below, the triangle's size and shape factors are plotted as functions of the time normalized by the largest eddy turnover time for the same particle drift velocities $0.4 \leq \gamma \leq 2$, St=2, and an initial separation Δ_0/η=92.5 in the same inertial subrange.

For a given initial separation, when the particle drift velocity increases, Figs. 10(a) and 11(a), the triangle's size is reduced, indicating smaller separations between the triangle's vertices. This happens because the increase of the gravity effect makes the particles stay together for longer times. A similar effect is observed in Figs. 10(b) and 11(b) for the shape factors $\langle W \rangle$ and $\langle I_2 \rangle$: with the increase of the particle drift velocity, it takes more time for the shape factor to reach its asymptotic value. Overall, the more gravity, the more memory there is for the triangle in terms of either size or shape. From Fig. 12, it can be seen that for the same drift velocity the shape factor reaches its asymptotic value faster when the inertia increases.

C. Effect of Re for particles with gravity

We study the effect of changing Re in the presence of gravity. The time evolution of the triangle's size and shape factor for different initial separations (Δ_0/L_1=0.0005, 0.032, and 0.5) are plotted for different drift velocities and different St. All the curves of $\langle R^2 \rangle^{1/2}$ and $\langle W \rangle$ for a constant value of Δ_0/L_1=0.032 and Δ_0/L_1=0.5, shown in Figs. 13–15, col-

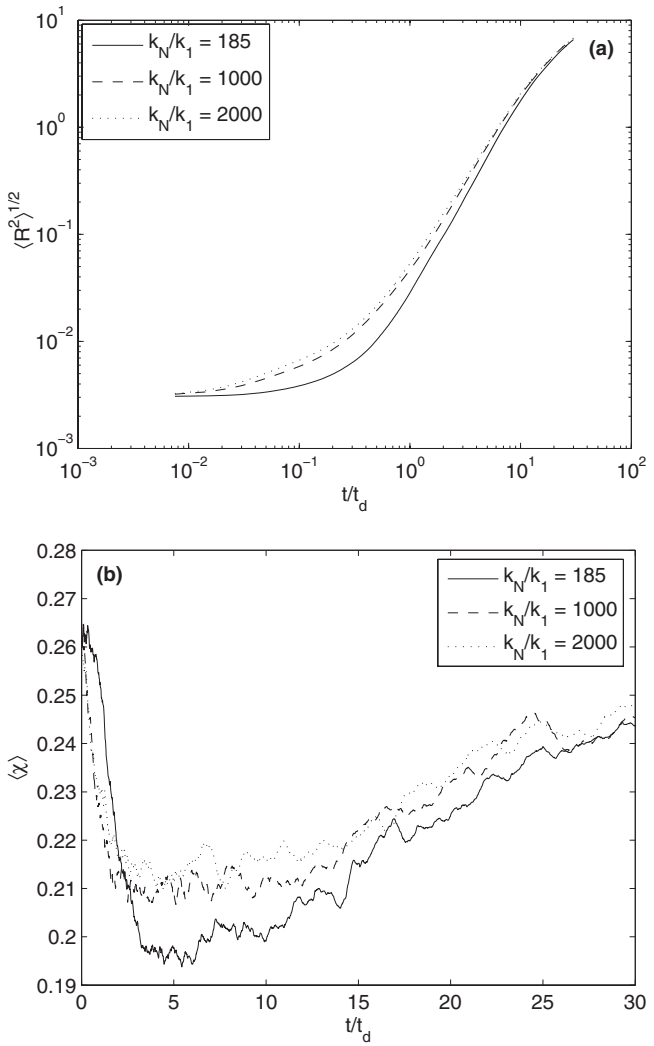

FIG. 16. Time evolution of (a) the triangle size and (b) the shape factor $\langle\chi\rangle$, for initial separation $\Delta_0/L_1=0.0005$, for particles with a drift velocity (for cases A2, M2, and T2 in Table II).

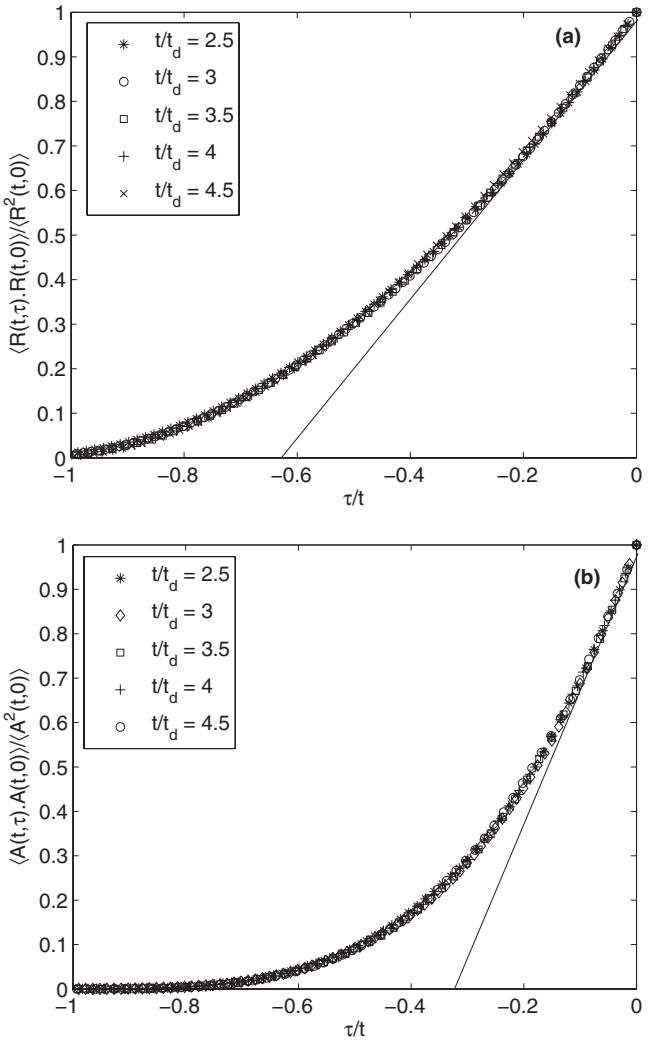

FIG. 17. Lagrangian correlation function of (a) the normalized triangle size and (b) the normalized triangle area at different times for case B2 in Table II.

lapse for a drift velocity in the range of $0.2\leq\gamma\leq2$ at two different St, St=0.02 and 2. These plots corresponds to different Re, but in all cases presented there $\Delta_0>\eta$. However, for the value of $\Delta_0/L_1=0.0005$, shown in Fig. 16, where the initial separation between the heavy particles lies below the Kolmogorov length scale, the curves of $\langle R^2\rangle^{1/2}$, $\langle W\rangle$, and $\langle\chi\rangle$ do not collapse.

Hence, we can conclude that Re has no effect on the size or shape of the triangle provided that the initial separation is larger than the Kolmogorov length scale. What matters is the portion L/Δ_0 of the inertial range that is contained in the initial triangle. This result has been known for fluid particles [2] but it was not obvious that it could be generalized to particles with inertia in the presence of gravity. So we can extend the results obtained in [2] for three fluid particles to three heavy particles, for particle drift velocities in the range of $0.2\leq\gamma\leq2$, St in the range $0.02\leq\mathrm{St}\leq2$, and inertial ranges $185\leq k_N/k_1\leq2000$, if the particles were initially separated by more than a Kolmogorov length scale η; then the size and shape of the triangle is independent of Re but a function of L/Δ_0.

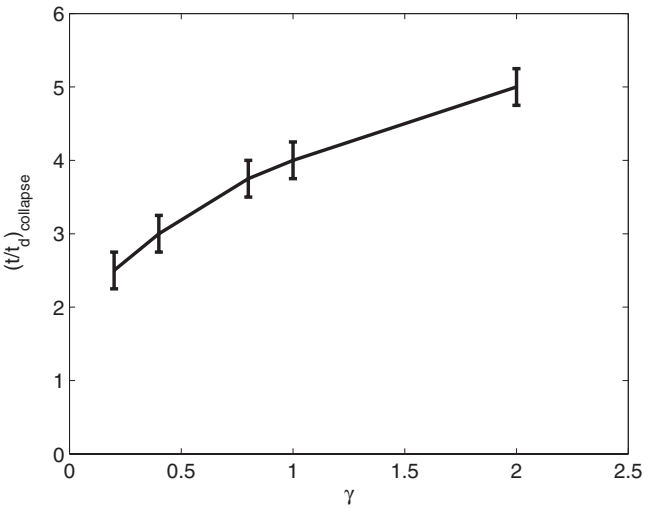

FIG. 18. Relation between particle drift velocity and the normalized time at which the Lagrangian correlation functions collapse.

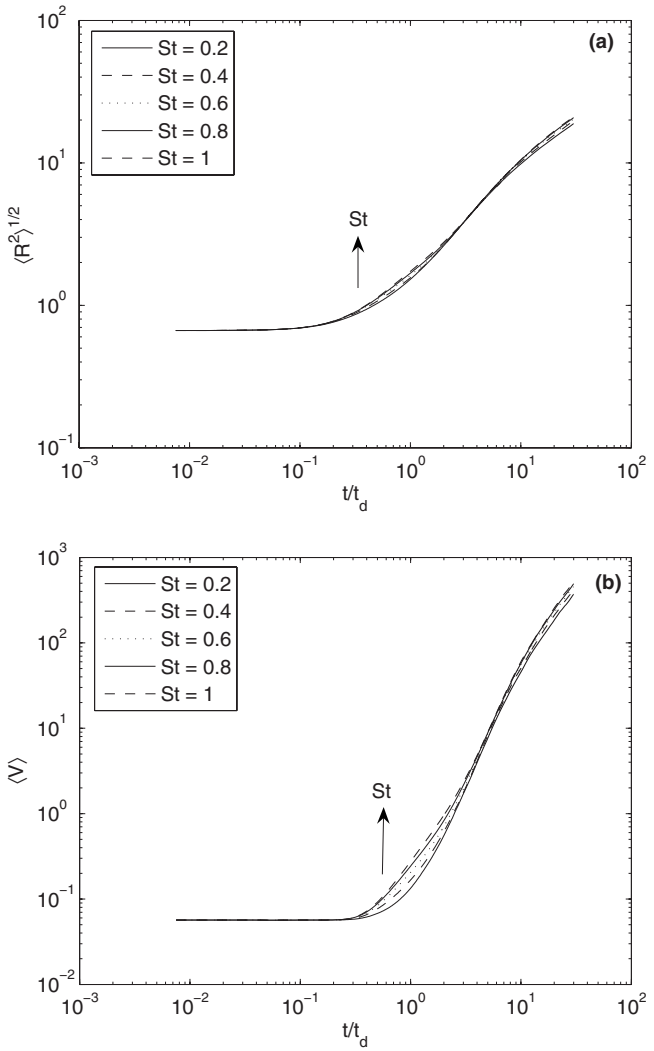

FIG. 19. Time evolution of (a) the tetrahedron size and (b) the tetrahedron volume $\langle V \rangle$, for particles with inertia (cases G1, H1, I1, J1, and K1 in Table I).

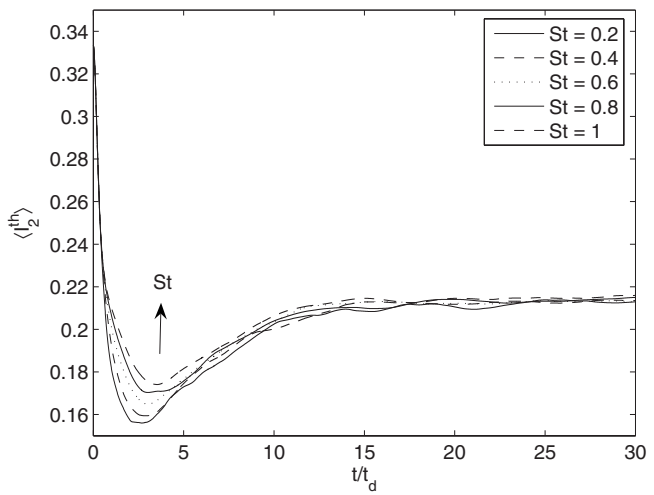

FIG. 20. Time evolution of the tetrahedron shape factor $\langle I_2^{th} \rangle$ for particles with inertia (cases G1, H1, I1, J1, and K1 in Table I).

TABLE IV. Comparisons of the values for the shape factors for three-particle sets.

Coefficient	KS with inertia	KS without inertia [2]	DNS simulation without inertia [4]	Gaussian values
$\langle I_2^{th} \rangle_{asy}$	0.21	0.215	0.21	0.222

1. The Lagrangian autocorrelation function in the presence of a particle with drift

KS is used to produce the Lagrangian correlation function of the three-heavy-particle set for the triangle normalized size R and the normalized triangle area A, Fig. 17. Figure 18 shows t/t_d after which the curves for the area correlation collapse as a function of the particle's drift velocity. The correlation time for the triangle size is found to be $C_S = 0.62$ (at the particle drift velocity $\gamma = 0.2$), indicating that the set vertices remember about 0.62 of their history, while

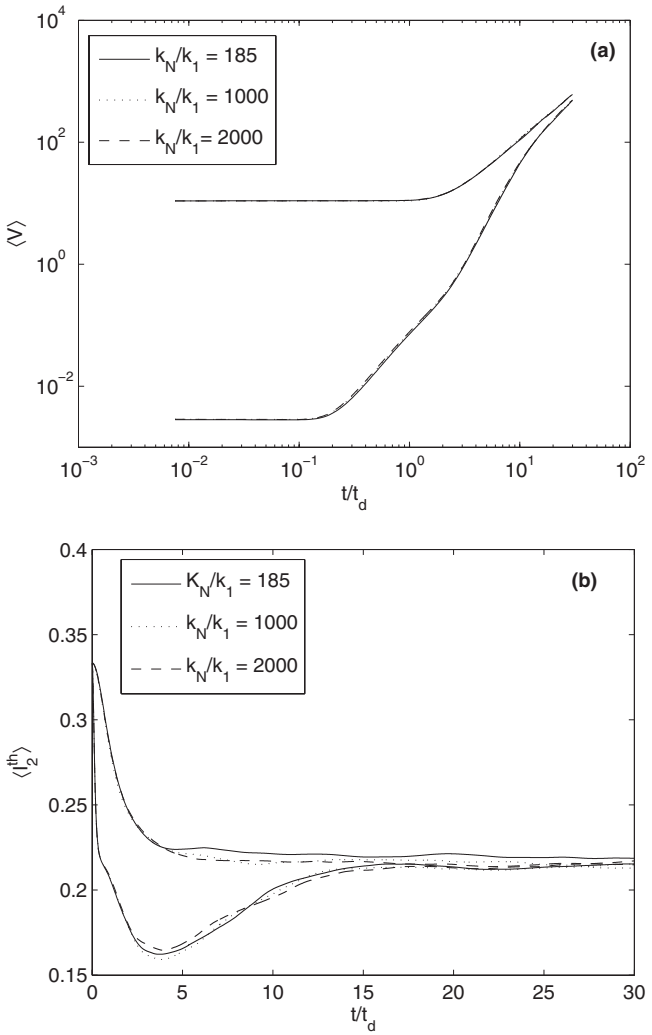

FIG. 21. Time evolution of (a) the tetrahedron volume $\langle V \rangle$ and (b) the tetrahedron shape factor $\langle I_2^{th} \rangle$, for (top) $\Delta_0/L_1 = 0.5$ and (bottom) $\Delta_0/L_1 = 0.032$, St=1, and different Re (cases F1, N1, P1, Q1, S1, and T1 in Table I).

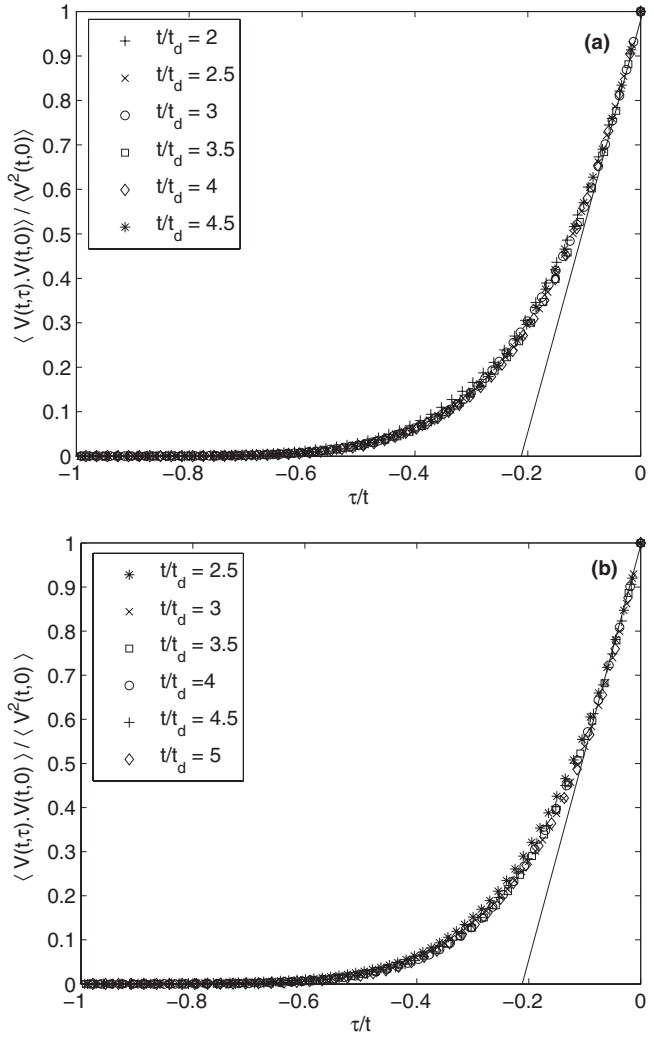

FIG. 22. Lagrangian correlation function of the normalized tetrahedron volume $\langle V \rangle$ at different times, (a) for case B1 in Table I and (b) for case C1 in Table I.

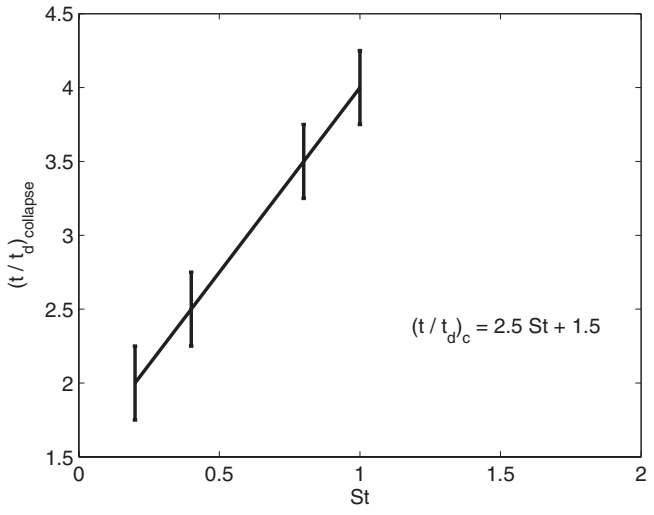

FIG. 23. Relation between St and the normalized time at which the Lagrangian correlation functions collapse.

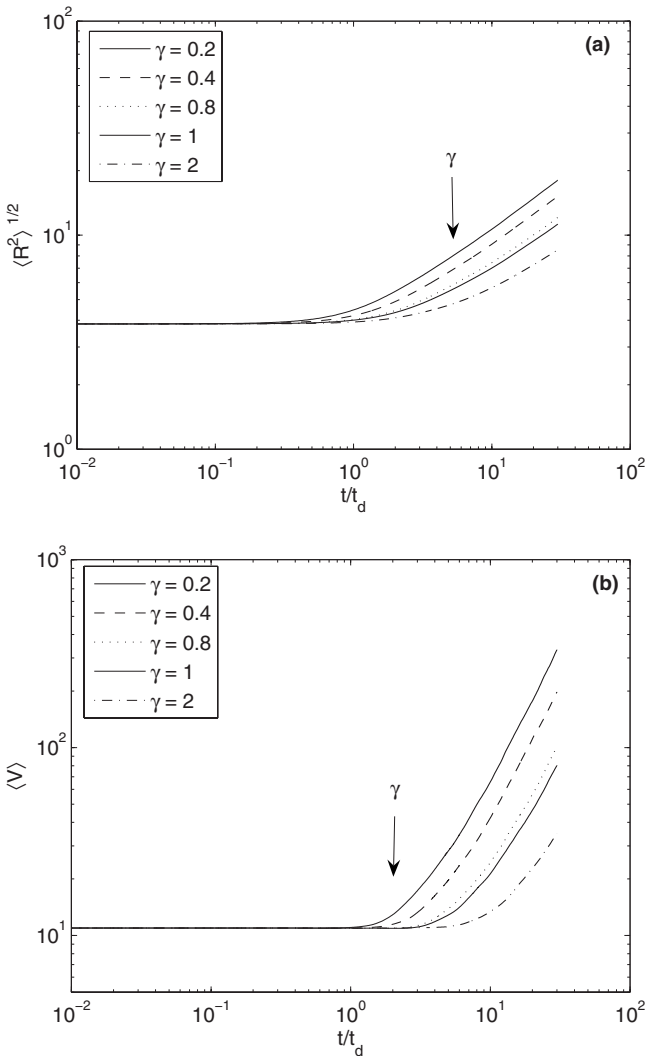

FIG. 24. Time evolution of (a) the tetrahedron size and (b) the tetrahedron volume for particles with drift, St=0.02, Δ_0/η=92.5, and k_N/k_1=185 (cases H2, I2, J2, K2, and L2 in Table II); from top to bottom γ=0.2, 0.4, 0.8, 1, and 2.

the correlation time for the triangle area is found to be C_A =0.35 for the three-heavy-particle set, which indicates that the set also remembers about 0.35 of its history; these two times are found to be independent of the particle drift velocity γ.

IV. RESULTS FOR FOUR-HEAVY-PARTICLE SETS

The effect of particle inertia and drift velocity on four-heavy-particle sets for different initial separations and different inertial ranges is presented here. The calculations are made for four-heavy-particle sets with different inertia (different St) with and without the gravity effect (different particle drift velocities), for different initial separations between the four particles and different inertial subranges of the turbulent flow field. The results obtained are in agreement with the general behavior observed in [2] for the case of diffusion.

A. Effect of particle inertia on a four-heavy-particle set

We first study the effect of the particle inertia (changing St values) in the absence of gravity (γ=0). The tetrahedron

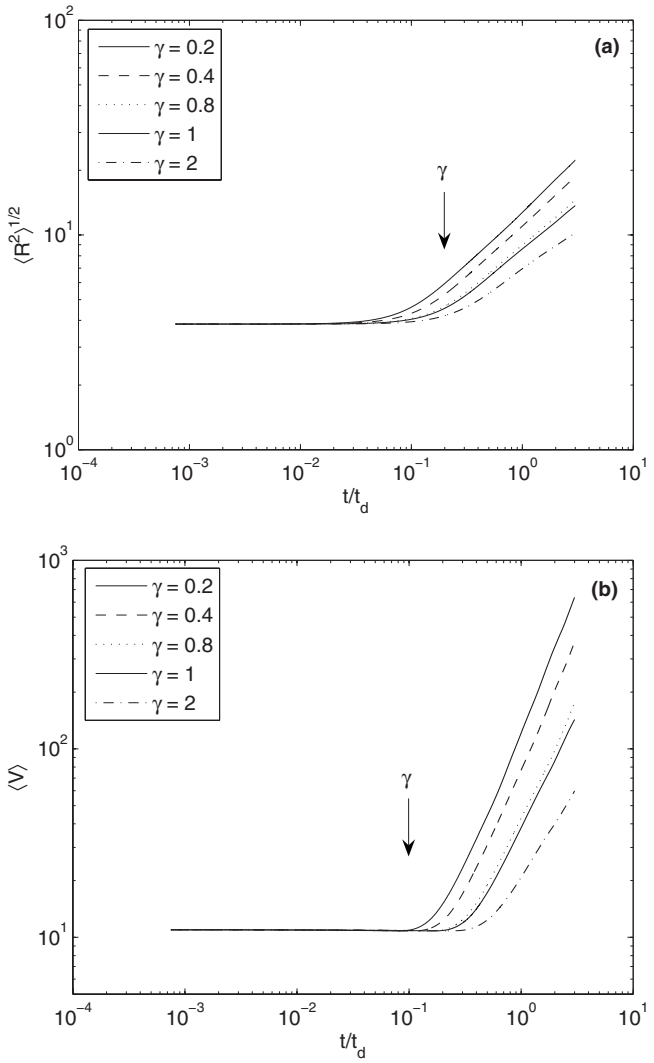

FIG. 25. Time evolution of (a) the tetrahedron size and (b) the tetrahedron volume for particles with drift, St=2, Δ_0/η=92.5, and k_N/k_1=185 (cases H2, I2, J2, K2, and L2 in Table II); from top to bottom γ=0.2, 0.4, 0.8, 1, and 2.

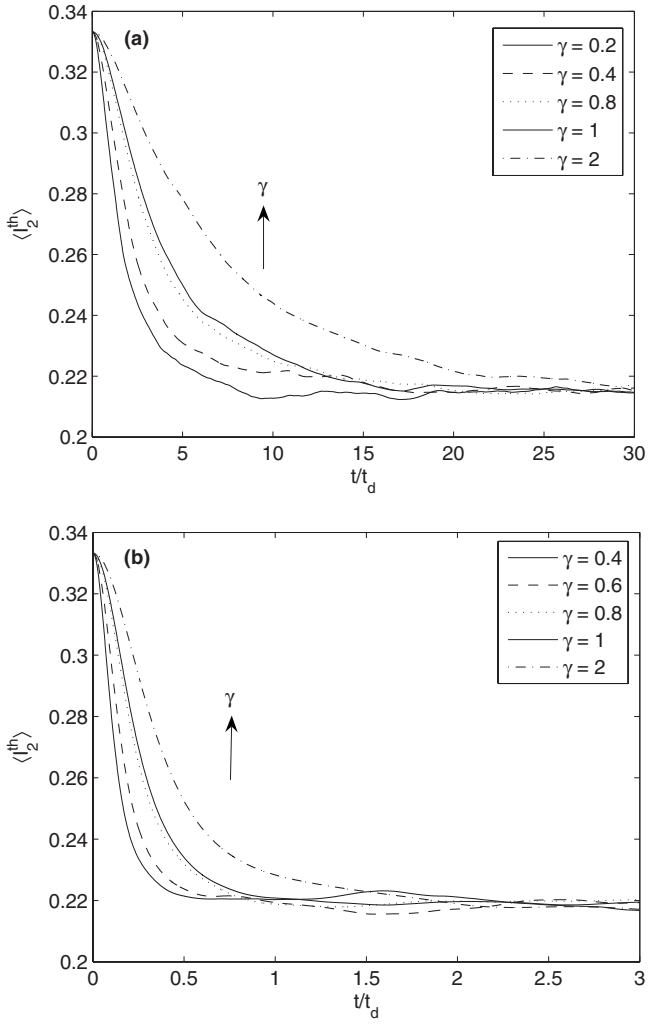

FIG. 26. Time evolution of the tetrahedron shape factor $\langle I_2^{\text{th}}\rangle$: (a) St= (a) 0.02 and (b) 2, Δ_0/η=92.5, and k_N/k_1=185 (cases H2, I2, J2, K2, and L2 in Table II); from bottom to top γ=0.2, 0.4, 0.8, 1, and 2.

size $\langle R^2\rangle^{1/2}$ and volume $\langle V\rangle$ are monitored as functions of time by computing their time evolution for different particle inertias. The change in the tetrahedron's shape is measured using the parameter $\langle I_2^{\text{th}}\rangle$ as a function of time.

1. Effect of varying St for a given initial separation

In this section, the effect of the particle inertia on the dispersion of the four heavy particles is studied for a given initial separation Δ_0/η=16 and a zero drift velocity. In Figs. 19 and 20, the evolution of the tetrahedron's size and shape is plotted for particles with inertia for different St.

The effect of varying St at the same initial separation on the tetrahedron's size can be seen in Fig. 19: when St increases the time needed before starting the Richardson regime is changed, and this duration increases with St. The effect of varying St, at a given initial separation, on the tetrahedron's shape can be seen in Fig. 20. When St increases, the local-minimum departure from the asymptotic value of the shape factor decreases. At large times, approximately at t/t_d=18, it directly reaches its asymptotic value without passing through a local minimum, $\langle I_2^{\text{th}}\rangle_{\text{asy}}$=0.215, in Fig. 20, which is in good agreement with the results from literature, Table IV. We can therefore extend the domain of validity of the values obtained in [4] and [2] for the dispersion of a four-heavy-particle set to St in the range $0.2 \leq \text{St} \leq 2$, at zero drift velocity.

2. Effect of the Re for particles with inertia

The results obtained for the tetrahedron's volume are plotted in Fig. 21 for two different initial separations, Δ_0/L_1 =0.032 and 0.5, St=1, and different Re. In all cases $\Delta_0 \geq \eta$.

All the curves for $\langle V\rangle$ and $\langle I_2^{\text{th}}\rangle$, for the two initial separations, collapse for the different Re. This result was obtained for the same case of four-particle sets in diffusion [2]. We can therefore extend it to the four-heavy-particle set dispersion for St in the range of $0.2 \leq \text{St} \leq 1$ at a zero drift velocity for inertial ranges $185 \leq k_N/k_1 \leq 2000$, and provided that $\Delta \geq \eta$.

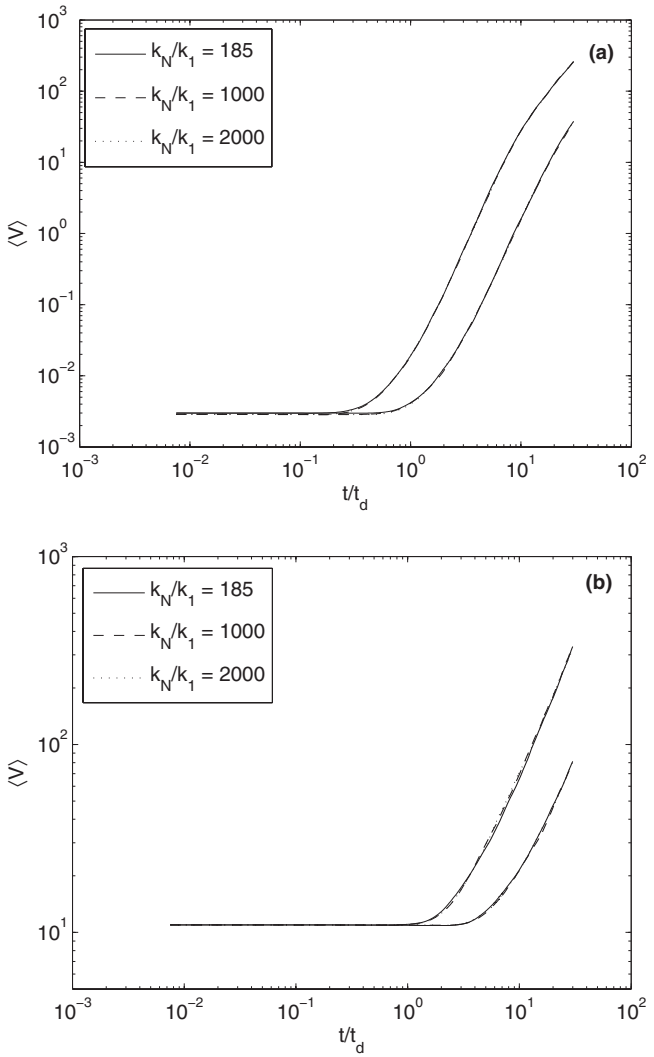

FIG. 27. Time evolution of the tetrahedron volume $\langle V \rangle$ for different Re: (a) $\Delta_0/L_1=0.032$, top curves $\gamma=0.2$ (cases F2, N2, and U2 in Table II), bottom curves $\gamma=1$ (cases G2, O2, and V2 in Table II); (b) $\Delta_0/L_1=0.5$, top curves $\gamma=0.2$ (cases H2, P2, and W2 in Table II), bottom curves $\gamma=1$ (cases K2, R2, and X2 in Table II).

3. The volume autocorrelation function in the presence of a particle with inertia

Lagrangian correlation functions for tetrahedrons in fluid diffusion were introduced in [2]. Here, we use KS to produce the Lagrangian correlation function of the tetrahedron volume (Fig. 22), but for four heavy particles to address the effect of the particle inertia. The correlation (e.g., for the volume) is defined as follows:

$$R(t,\tau) = \langle V(t+\tau)V(t,0)\rangle / \langle V^2(t,0)\rangle. \tag{22}$$

Figure 23 shows the time t/t_d after which the curves for the volume correlation collapse. The figure indicates a linear relation between this time and St. The correlation time is found to be $C_V=0.21$, which indicates that the set remembers about 0.21 of its history; this value is found to be constant and does not depend on St.

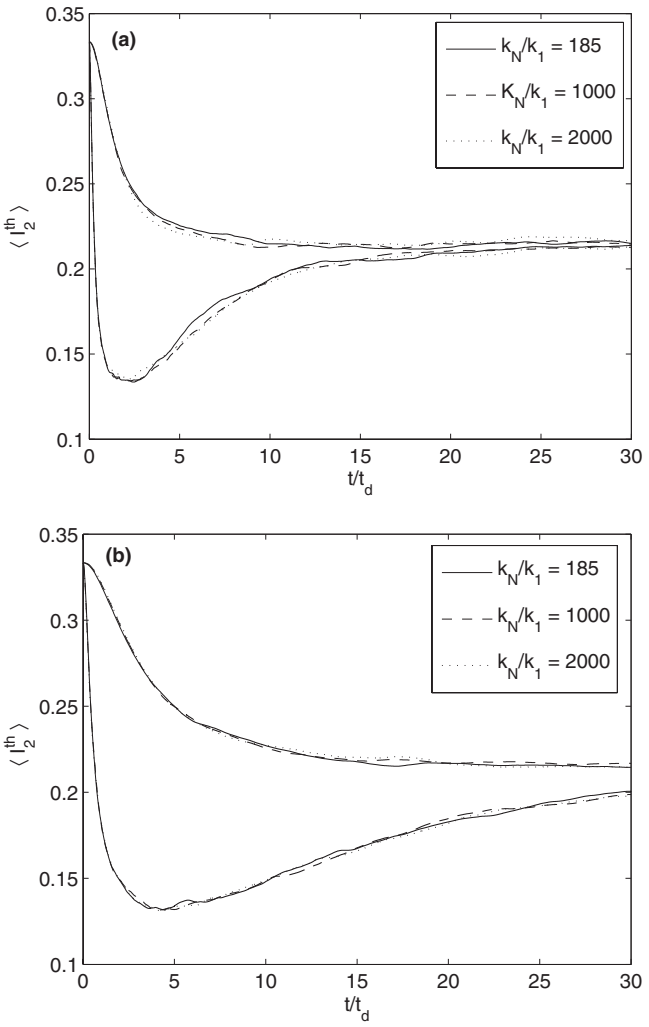

FIG. 28. Time evolution of the tetrahedron shape factor $\langle I_2^{\text{th}} \rangle$ for different Re (a) $\gamma=0.2$; top curves for an initial separation $\Delta_0/L_1=0.5$ (cases H2, P2, and W2 in Table II), bottom curves for an initial separation $\Delta_0/L_1=0.032$ (cases F2, N2, and U2 in Table II); (b) $\gamma=1$; top curves for an initial separation $\Delta_0/L_1=0.5$ (cases K2, R2, and X2 in Table II), bottom curves for an initial separation $\Delta_0/L_1=0.032$ (cases G2, O2, and V2 in Table II).

B. Effect of particle drift velocity on a four-heavy-particle set

In this section, we consider the effect of gravity in the presence of particle inertia on the dispersion of four-heavy-particle sets. The evolution of the size and geometry of an initially equilateral tetrahedron is presented. The volume of the tetrahedron is recorded as a function of time by computing the evolution of $\langle V \rangle$ and the changes in the tetrahedron's shape are measured using the parameter $\langle I_2^{\text{th}} \rangle$ as functions of time.

1. Effect of varying the drift velocity for a given initial separation

The evolution of the size and geometry of an initially equilateral tetrahedron immersed in an isotropic turbulent flow are studied for a given drift velocity at a fixed particle inertia (St) and fixed initial separation. The evolution of the

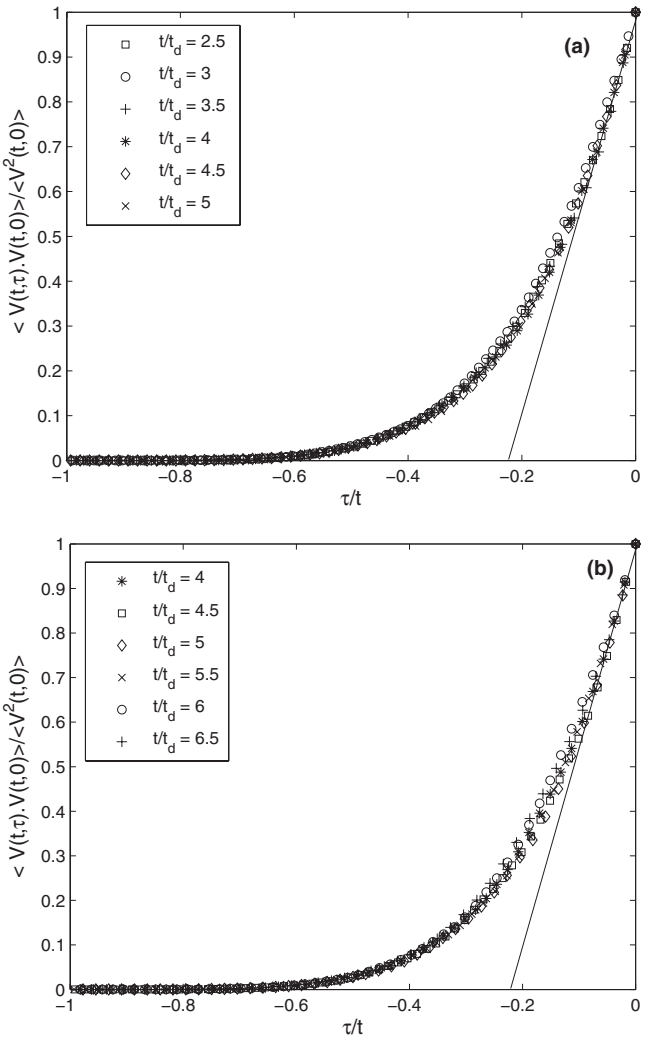

FIG. 29. Lagrangian correlation function of the tetrahedron volume: (a) case B2 in Table II and (b) case C2 in Table II at different times.

tetrahedron size and shape are plotted in Figs. 24 and 26 for different cases.

Figure 25 shows that at a given time, when the drift coefficient increases, the tetrahedron size is reduced indicating lower separations within the tetrahedron vertices. This is because the increase in the weight makes the particles move faster in the direction of the gravity, making them bypass part of the turbulent flow structures.

For the shape factor, Fig. 26, it can be noticed that when the drift coefficient decreases the shape factor reaches its asymptotic value faster. Whereas, when inertia increases [Fig. 26(b)] (St=2) the effect of increasing the drift cannot be counteracted. In this case the tetrahedron can get more distorted because it faces the combined effect of inertia, which tends to move the particles apart from the fluid element trajectories by the centrifugal effect, and of gravity, which tends to move the particles faster in the vertical direction. The resulting effect is a faster convergence to the Gaussian asymptotic values for the size and shape factor.

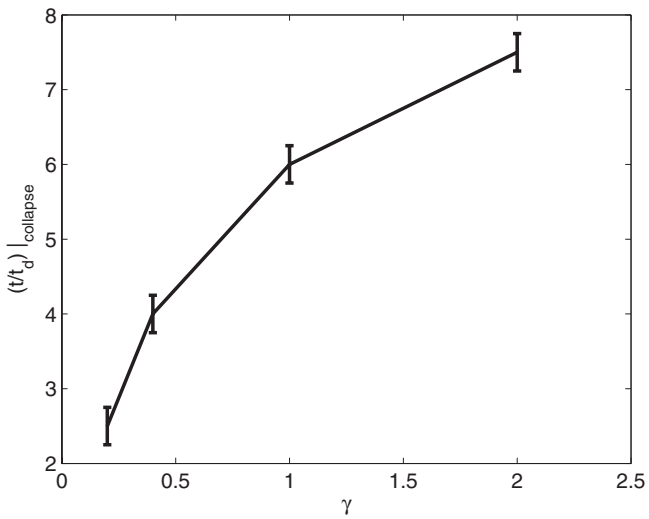

FIG. 30. Relation between particle drift velocity and the normalized time at which the Lagrangian correlation functions collapse.

2. Effect of Re for particles with gravity

The effect of Re in the presence of gravity is studied at a given drift velocity and for the two initial separations $\Delta_0/L_1=0.5$ and 0.032. All the curves for $\langle V\rangle$ and $\langle I_2^{\text{th}}\rangle$, for each separation $\Delta_0/L_1=0.032$ and 0.5, as shown in Figs. 27 and 28, collapse for a drift coefficient $0.2\leq\gamma\leq2.0$ at St $=0.02$. These results are in agreement with those obtained in Sec. III for inertia only and also with those obtained for four-fluid-particle diffusion [2]. We can therefore extend these results to the heavyparticle tetrahedron to drift velocities in the range $0.2\leq\gamma\leq2$, St=0.02, and inertial ranges $185\leq k_N/k_1\leq2000$.

3. Volume autocorrelation function in the presence of particles with gravity

Here, we study the effect of gravity on the Lagrangian correlation function of heavy particle tetrahedron volume (Fig. 29). Figure 30 shows t/t_d, the normalized time after which the curves for the volume correlation collapse as a function of the particle's drift velocity. The correlation time is found to be $C_V=0.22$ for a heavy particle tetrahedron, which indicates that the set remembers about 0.22 of its history; this factor is found to be constant and does not depend on the particle drift velocity γ.

V. CONCLUSION

In this paper, we study the effects of the particle inertia and weight on the dispersion of three- and four-heavy-particle sets in homogeneous isotropic turbulent flows. We follow the evolution of the size and shape of initially equilateral sets for different values of Re.

We can conclude that Re has no effect on the size or shape of heavy particle triangles or tetrahedrons, provided that the initial separation is larger than the Kolmogorov length scale.

What matters is the portion L/Δ_0 of the inertial range that is contained in the initial triangle or tetrahedron. This result has been known for fluid particles [2] but it was not obvious that it could be generalized to particles with inertia in the presence of gravity. Our results show that inertia has no effect on the asymptotic values of the shape factor for heavy particle triangles or tetrahedrons for St in the range $0.2 \leq \mathrm{St} \leq 2$, drift velocities in the range $0.2 \leq \gamma \leq 2$, and inertial subranges $185 \leq k_N/k_1 \leq 2000$. We can extend the validity of the values obtained in [2] (0.66 for $\langle W \rangle$, 0.16 for $\langle I_2 \rangle$, and 0.26 for $\langle \chi \rangle$) to the dispersion of three-heavy-particle sets in the case of varying St at a zero drift velocity.

[1] P. Castiglione and A. Pumir, Phys. Rev. E **64**, 056303 (2001).
[2] F. Nicolleau and A. ElMaihy, Phys. Rev. E **74**, 046302 (2006).
[3] L. Mydlarski, A. Pumir, B. I. Shraiman, E. D. Siggia, and Z. Warhaft, Phys. Rev. Lett. **81**, 4373 (1998).
[4] A. Pumir, B. I. Shraiman, and M. Chertkov, Phys. Rev. Lett. **85**, 5324 (2000).
[5] M. A. I. Khan, A. Pumir, and J. C. Vassilicos, Phys. Rev. E **68**, 026313 (2003).
[6] J. Cressman, J. Davoudi, W. Goldburg, and J. Schumacher, New J. Phys. **6**, 53 (2004).
[7] F. Nicolleau, K.-S. Sung, and J. C. Vassilicos (to be published).
[8] G. K. Batchelor, *The Theory of Homogeneous Turbulence*, 1st ed. (Cambridge University Press, Cambridge, UK, 1953).
[9] J. C. H. Fung, J. C. R. Hunt, and R. J. Perkins, Proc. R. Soc. London, Ser. A **459**, 445 (2003).
[10] N. A. Malik and J. C. Vassilicos, Phys. Fluids **11**, 1572 (1999).
[11] F. Nicolleau and J. C. Vassilicos, Phys. Rev. Lett. **90**, 024503 (2003).
[12] P. Flohr and J. C. Vassilicos, J. Fluid Mech. **407**, 315 (2000).
[13] A. ElMaihy and F. Nicolleau, Phys. Rev. E **71**, 046307 (2005).
[14] J. C. H. Fung, Ph.D. thesis, University of Cambridge, 1990.
[15] M. R. Maxey and J. J. Riley, Phys. Fluids **26**, 883 (1983).
[16] M. R. Maxey, E. Chang, and L.-P. Wang, Exp. Therm. Fluid Sci. **12**, 417 (1996).
[17] M. R. Maxey, B. Patel, E. Chang, and L.-P. Wang, Fluid Dyn. Res. **20**, 143 (1997).
[18] M. Chertkov, A. Pumir, and B. I. Shraiman, Phys. Fluids **11**, 2394 (1999).